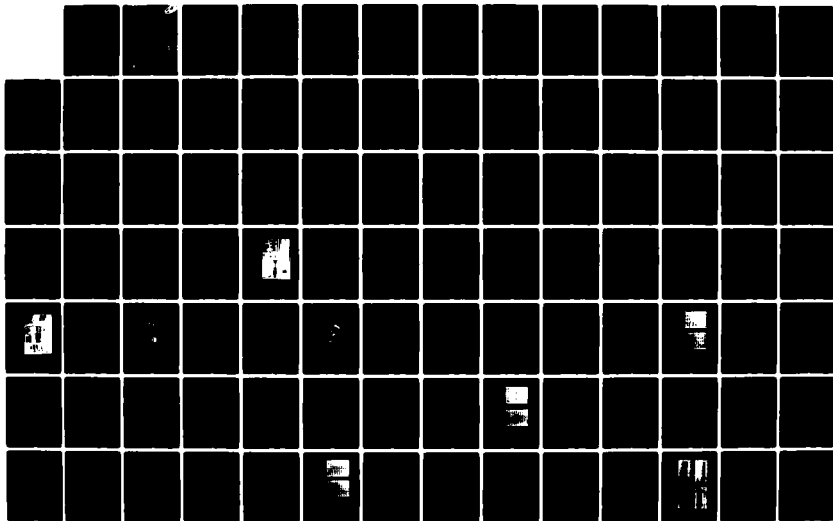AD-A131 350   NONLINEAR ELASTIC BEHAVIOR OF PIEZOELECTRIC TRIGONAL   1/2
               CRYSTALS: MEASUREMEN..(U) TENNESSEE UNIV KNOXVILLE DEPT
               OF PHYSICS P J LATIMER JUN 83 TR-23 N00014-81-K-0229
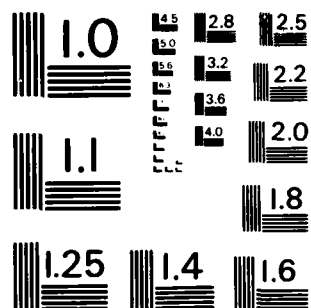UNCLASSIFIED   F/G 9/1   NL

MICROCOPY RESOLUTION TEST CHART

NATIONAL BUREAU OF STANDARDS – 1963 – A

AD A131350

OFFICE OF NAVAL RESEARCH
CONTRACT NO. N00014-81-K-0229
PROJECT NO. 384-306

M. A. Breazeale, Principal Investigator

NONLINEAR ELASTIC BEHAVIOR OF PIEZOELECTRIC
TRIGONAL CRYSTALS: MEASUREMENTS ON
QUARTZ AND LiNbO$_3$

by

Paul Jerry Latimer

DTIC
ELECTE
AUG 16 1983

D

TECHNICAL REPORT NO. 23

OFFICE OF NAVAL RESEARCH
CONTRACT NO. N00014-81-K-0229
PROJECT NO. 384-306

M. A. Breazeale, Principal Investigator

NONLINEAR ELASTIC BEHAVIOR OF PIEZOELECTRIC
TRIGONAL CRYSTALS: MEASUREMENTS ON
QUARTZ AND $LiNbO_3$

by

Paul Jerry Latimer

Ultrasonics Laboratory
Department of Physics
The University of Tennessee
Knoxville, Tennessee 37996-1200

June 1983

Distribution of This Document is Unlimited

DTIC
ELECTE
S
AUG 1 5 1983
D

D

REPORT DOCUMENTATION PAGE		READ INSTRUCTIONS BEFORE COMPLETING FORM
1. REPORT NUMBER Technical Report 23	2. GOVT ACCESSION NO. AD-A131350	3. RECIPIENT'S CATALOG NUMBER
4. TITLE (and Subtitle) NONLINEAR ELASTIC BEHAVIOR OF PIEZOELECTRIC TRIGONAL CRYSTALS: MEASUREMENTS ON QUARTZ AND LiNbO$_3$		5. TYPE OF REPORT & PERIOD COVERED Interim
		6. PERFORMING ORG. REPORT NUMBER
7. AUTHOR(s) Paul Jerry Latimer		8. CONTRACT OR GRANT NUMBER(s) N00014-81-K-0229
9. PERFORMING ORGANIZATION NAME AND ADDRESS Department of Physics The University of Tennessee Knoxville, TN 37996-1200		10. PROGRAM ELEMENT, PROJECT, TASK AREA & WORK UNIT NUMBERS
11. CONTROLLING OFFICE NAME AND ADDRESS Office of Naval Research, Code 412 Department of the Navy Arlington, VA 22217		12. REPORT DATE June 1983
		13. NUMBER OF PAGES 106
14. MONITORING AGENCY NAME & ADDRESS(if different from Controlling Office)		15. SECURITY CLASS. (of this report) Unclassified
		15a. DECLASSIFICATION/DOWNGRADING SCHEDULE

16. DISTRIBUTION STATEMENT (of this Report)

Approved for public release; distribution unlimited.

17. DISTRIBUTION STATEMENT (of the abstract entered in Block 20, if different from Report)

18. SUPPLEMENTARY NOTES

19. KEY WORDS (Continue on reverse side if necessary and identify by block number)
nonlinear wave propagation
nonlinearity of trigonal crystals
harmonic generation
nonlinear distortion of ultrasonic waves in solids
TOE constants of trigonal crystals

20. ABSTRACT (Continue on reverse side if necessary and identify by block number)
The ultrasonic harmonic generation technique previously used to measure third-order elastic (TOE) constants of crystals of cubic symmetry has been extended to measurement of crystals of trigonal symmetry. The theory for nonpiezo-electric trigonal crystals of J. Philip [Technical Report No. 22, Office of Naval Research, Contract No. N00014-81-K-0229 (to be published in 1983)] has been combined with the piezoelectric theory of McMahon [J. Acoust. Soc. Am. 44, 1007 (1968)] to determine the effective TOE constants in a piezoelectric solid, and a correction has been made to McMahon's expression.

DD $_{1 \text{ JAN } 73}^{\text{FORM}}$ 1473   EDITION OF 1 NOV 65 IS OBSOLETE
S/N 0102-LF-014-6601

(20) continued

Measurements in weakly piezoelectric quartz have produced values of C_{111} and C_{333} which agree within experimental uncertain with values of R. N. Thurston, H. J. McSkimin and P. Andreatch, Jr. [J. Appl. Phys. 37, 267 (1966)] and R. Stern and R. T. Smith [J. Acoust. Soc. Am. 44, 640 (1968)] after corrections have been made for the effect of diffraction on the data. Measurements in strongly piezoelectric $LiNbO_3$ have resulted in values which agree reasonably well with those of J. Philip and M. A. Breazeale [Proc. IEEE Ultrasonics Symposium, Vol. 2 (1982)] but disagree with those of C. Y. Nakagawa, K. Yamanouchi and K. Shibayama [J. Appl. Phys. 44, 3969 (1973)]. There is indication of some sample dependence of the values of both the second-order elastic constants as well as the third-order elastic constants of $LiNbO_3$ samples currently available.

In the course of measurement of the TOE constants a negative nonlinearity parameter was observed for the piezoelectric [100] direction in quartz. This peculiarity is impossible for thermodynamic reasons in fluids, but has been observed once previously in fused silica [J. Bains and M. A. Breazeale, J. Acoust. Soc. Am. 57, 745 (1975)]. The nonlinearity parameter appears to be positive for the piezoelectric [001] direction in $LiNbO_3$.

The data presented are for the "piezoelectrically stiffened" TOE constants; however, there are preliminary indications that the harmonic generation technique may give access to the constant field TOE constants $c_{ijk}^{(E)}$.

NONLINEAR ELASTIC BEHAVIOR OF PIEZOELECTRIC TRIGONAL

CRYSTALS: MEASUREMENT ON QUARTZ AND $LiNbO_3$

by

Paul Jerry Latimer

TECHNICAL REPORT NO. 23

Ultrasonics Laboratory
Department of Physics
The University of Tennessee
Knoxville, Tennessee 37996-1200

June 1983

PREFACE

This report is an adaptation of the dissertation of Paul Jerry Latimer submitted to the Department of Physics at The University of Tennessee in partial fulfillment of the requirements of the degree of Doctor of Philosophy.

The ultrasonic harmonic generation technique previously used to measure third-order elastic (TOE) constants of crystals of cubic symmetry has been extended to measurement of crystals of trigonal symmetry. The theory for nonpiezoelectric trigonal crystals of J. Philip [Technical Report No. 22, Office of Naval Research, Contract No. N00014-81-K-0229 (to be published in 1983)] has been combined with the piezoelectric theory of McMahon [J. Acoust. Soc. Am. $\underline{44}$, 1007 (1968)] to determine the effective TOE constants in a piezoelectric solid, and a correction has been made in McMahon's expression.

Measurements in weakly piezoelectric quartz have produced values of C_{111} and C_{333} which agree within experimental uncertainty with values of R. N. Thurston, H. J. McSkimin and P. Andreatch, Jr. [J. Appl. Phys. $\underline{37}$, 267 (1966)] and R. Stern and R. T. Smith [J. Acoust. Soc. Am. $\underline{44}$, 640 (1968)] after corrections have been made for the effect of diffraction on the data. Measurements in strongly piezo-electric $LiNbO_3$ have resulted in values which agree reasonably well with those of J. Philip and M. A. Breazeale [Proc. IEEE Ultrasonics Symposium, Vol. 2 (1982)] but disagree with those of C. Y. Nakagawa, K. Yamanouchi and K. Shibayama [J. Appl. Phys. $\underline{44}$, 3969 (1973)].

There is indication of some sample dependence of the values of both the second-order elastic constants as well as the third-order elastic constants of LiNbO$_3$ samples currently available.

In the course of measurement of the TOE constants a negative nonlinearity parameter was observed for the piezoelectric [100] direction in quartz. This peculiarity is impossible for thermodynamic reasons in fluids, but has been observed once previously in fused silica [J. Bains and M. A. Breazeale, J. Acoust. Soc. Am. 57, 745 (1975)]. The nonlinearity parameter appears to be positive for the piezoelectric [001] direction in LiNbO$_3$.

The data presented are for the "piezoelectrically stiffened" TOE constants; however, there are preliminary indications that the harmonic generation technique may give access to the constant field TOE constants $C_{ijk}^{(E)}$.

TABLE OF CONTENTS

LIST OF TABLES

LIST OF FIGURES

CHAPTER I

INTRODUCTION

Over the past several years it has become increasingly evident that a linear theory is inadequate to give a detailed accounting of the properties of solids. Many basic properties of solids can be explained only on the basis of nonlinear theory. Among these properties are thermal expansion, interaction of lattice waves, inequality of adiabatic and isothermal elastic constants, and the dependence of the elastic constants on pressure and temperature.

The description of the nonlinear properties of solids is made in terms of the higher-order elastic constants. The elastic constants are the coefficients of the terms of a series expansion of the strain energy per unit volume of the solid in powers of the strains. The coefficients of the second powers in strains are the ordinary elastic constants which appear in linear theories and the coefficients of the third powers in strain are the third-order elastic (TOE) constants which are the subject of this dissertation. This is a problem of funda- mental interest to solid state physics: the measurement of higher- order elastic constants and the correlation of their magnitude with physical properties. Technological implications are important as well.

The second-order elastic (SOE) constants are determined directly from the measurement of the velocity of the ultrasonic waves in the solid; the TOE constants must be measured by a combination of at least two techniques.

1

Measurement of the dependence of second-order elastic constants on hydrostatic pressure gives combinations of third-order elastic constants but does not give the complete set for a particular crystal symmetry. Lazarus (1949) measured the pressure dependence of SOE constants of NaCl, KCl, CuZn, Cu, and Al. Hearmon (1953) using equations obtained by Birch (1947) determined the combination of TOE constants which could be calculated from Lazarus' data.

To determine a complete set of TOE constants, one can in addition evaluate the change in ultrasonic wave velocity with uniaxial stress. This technique, which has some inherent shortcomings, does give a complete set of TOE constants if the data are used in combination with hydrostatic pressure measurements. The first complete set of TOE constants for an isotropic material was made by Hughes and Kelly (1953) by measuring the change of ultrasonic wave velocity with hydrostatic pressure and with uniaxial stress in polystyrene and plexiglass. Seeger and Buck (1960) developed a theory for sound velocities in crystals subject to hydrostatic pressure and uniaxial stress in terms of SOE and TOE constants for cubic crystals. Bateman, Mason and McSkimin (1961) performed measurements on germanium and obtained the first complete set of six TOE constants of a cubic crystal. Since that time measurements have been made on a large number of cubic crystals using the uniaxial stress and hydrostatic pressure derivatives.

The other technique which has been widely used to measure the TOE constants of solids is the ultrasonic harmonic generation

technique described by Breazeale and Thompson (1963) and independently

by Gedroits and Krasilnikov (1963). Breazeale and Ford (1965) solved

the nonlinear equation of motion for the case of isotropic solids and

cubic crystals. Gauster and Breazeale (1966) developed the capacitive

receiver which is capable of yielding a combination of TOE constants

from the absolute amplitudes of the fundamental and second harmonic

of a finite amplitude ultrasonic wave as it propagates through a non-

linear solid. Since that time many measurements have been made for

cubic crystals using this technique as reported in a comprehensive

review by Breazeale and Philip (1983). Very few measurements of TOE

constants have been reported for crystals in the trigonal group. As

the symmetry becomes lower (Hearmon, 1979), the number of elastic con-

stants increases. For example, crystals belonging to the 3m, 32, 3m

class in the trigonal symmetry group have 14 TOE constants. McMahon

(1968) developed a nonlinear theory for the evaluation of certain

TOE constants of piezoelectric solids by second harmonic generation.

In his theory McMahon evaluates the effect of piezoelectric "stiffen-

ing" upon both the SOE and TOE constants. He shows that the overall

effect of piezoelectricity is to increase the magnitude of both the

SOE and TOE constants. He then evaluates the effective constants in

terms of other higher-order constants of the material. Philip (1983)

extended the linear theory for nonpiezoelectric solids in a very

general way such that the nonlinear distortion of finite amplitude

waves could be described in the case of trigonal symmetry by a

perturbation solution of the nonlinear equation.

Of the work done on crystals with trigonal symmetry, the hydrostatic and uniaxial stress derivatives of ultrasonic wave velocity is the technique which has been used almost exclusively. To the author's knowledge, no previous harmonic generation measurements have been performed with the capacitive detector on a material with trigonal symmetry—except for some preliminary measurements made by Philip and Breazeale (1982) on lithium niobate.

The first full set of TOE constants for a trigonal crystal was measured by Thurston et al. (1966). They used the hydrostatic pressure uniaxial stress derivative technique to determine the 14 TOE constants of quartz. Quartz is a weakly coupled piezoelectric material in which the effect of acoustical variation of the electrical conditons does not make a perceptible change in the measured value of the elastic constants. Thurston et al. (1966) claimed that the piezo-electric coupling is weak enough that the effect on their measure-ments was within experimental error, and therefore they made no distinction between the TOE constants at constant electric field and the effective TOE constants they measured.

Stern and Smith (1968) measured the TOE constants of quartz using a pulse echo interferometer technique, a modification of the uniaxial stress-hydrostatic pressure derivative technique. Their values were in good agreement with those of Thurston et al. (1966).

A microwave ultrasonic harmonic generation technique has been used by Carr (1968) to determine the TOE constants C_{111} and C_{333} of quartz and sapphire. The technique consisted of generating a

microwave ultrasonic fundamental at one end of the sample and detecting the second harmonic at the other end by the piezoelectric effect. The quantitative measurements of the second harmonic led to a determination of the TOE constants. Even though C_{111} for both samples agreed reasonably well with other published data, Carr's value for C_{333} appeared to be considerably greater in magnitude than other measurements.

Graham (1972) described a method for obtaining longitudinal TOE constants of X-cut quartz: Solids are subjected to shock wave loading and undergo compression. The shock compression data were analyzed to determine C_{111} and C_{1111} for X-cut quartz. The determination of the TOE constants under these large compressions allows one to test the applicability of the finite strain formulation of the constitutive relations.

The 14 TOE constants of trigonal Al_2O_3 were measured by Hankey and Schuele (1970). They measured hydrostatic pressure and uniaxial stress dependence of the ultrasonic wave velocity by the pulse echo technique.

Kaga (1968) measured the TOE constants of trigonal calcite using a pulse-superposition technique with uniaxial stress and hydrostatic pressure.

The TOE constants of the strongly coupled piezoelectric trigonal $LiNbO_3$ crystal were measured by Nakagawa et al. (1973). A pulse transmission technique was used to determine the velocity of small amplitude ultrasonic waves as a function of applied stress. Piezoelectric

terms were included in the calculation of pressure derivatives of sound velocity in terms of the TOE constants developed by Thurston and Brugger (1965); however, lack of piezoelectric coefficients prevented evaluation of the constant field TOE constants $C_{ijk}^{(E)}$. Hearmon (1979) erroneously reported that the TOE constants measured by Nakagawa et al. (1973) were constant field coefficients. However, Hearmon (1979) was correct in pointing out that the measurement errors reported by Nakagawa et al. was sufficiently large that they cast some doubt on the validity of the data. In particular, the errors were largest for C_{111} and C_{333}. These are the TOE constants which are directly measured by the technique described in this thesis.

The measurements reported in this study were made on trigonal crystals with the capacitive receiver. They allow a direct determination of the coefficients C_{111} and C_{333} in trigonal crystals. One objective in reporting the measurements is to experimentally verify the theory of Philip (1983) for trigonal crystals. In addition, the theory has been expanded to account for the effect of piezoelectricity on the harmonic generation measurements. The expansion of the theory closely parallels McMahon's derivation of an expression for the effective elastic constant for piezoelectric materials, but corrects an error in the final expression by McMahon (1965), an error that was repeated in the derivation of the next higher order terms by Mathur and Gupta (1970).

The effect of diffraction on the measurements also is considered. It is found that even with the large (1" diameter, 1.5" long) samples

and a D/λ ratio of the order of 75, the effect of diffraction, calculated by the procedure described by Blackburn (1981) cannot be ignored.

Finally, the nonlinear behavior of the weakly coupled piezoelectric trigonal quartz is compared with the behavior of strongly coupled piezoelectric trigonal $LiNbO_3$.

CHAPTER II

THEORETICAL CONSIDERATIONS

The theory of second harmonic generation in trigonal crystals can be developed in a general way, as shown by Philip (1983). The piezoelectric relations can be derived by making some modifications of the treatment of McMahon (1968) to make it more thermodynamically correct (Brugger, 1964). In effect, the present work merges the theories of Philip and McMahon to yield a suitable composite theory for the treatment of piezoelectric crystals of trigonal symmetry.

A. GENERAL THEORY OF NONLINEAR WAVE PROPAGATION IN SOLIDS

Consider a point P in the medium with coordinates a_i (a,b,c) in the unstrained state (Philip, 1983). Let P move to P' with coordinates x_i (x,y,z) in the deformed state.

The components of the displacement can then be written as

$$u = x - a$$
$$v = y - b$$
$$w = z - c . \tag{1}$$

In the Lagrangian formulation, the strain is described in terms of the initial or undeformed state, and the initial coordinates a_i of the material particle are taken as independent variables. The Lagrangian formulation is used exclusively in this development.

The Lagrangian strain parameters which are components of the finite strain tensor are given (Murnaghan, 1951) by

$$\eta = \frac{1}{2} (J^* J - I) \qquad (2)$$

where J is the Jacobian matrix given by

$$J = \begin{vmatrix} 1 + u_a & u_b & u_c \\ v_a & 1 + v_b & v_c \\ w_a & w_b & 1 + w_c \end{vmatrix} \qquad (3)$$

and where $u_a = \frac{\partial u}{\partial a}$, $u_b = \frac{\partial u}{\partial b}$, etc., J^* is the transpose of J, and I is the unit matrix.

Let $\phi(\eta)$ be the strain energy per unit of undeformed volume. The properties of the crystalline medium enter into the theory through the strain energy $\phi(\eta)$ which can be expressed in terms of the ordinary elastic constants by proper rotation of the coordinates

$$\phi(\eta) = \phi_0 + C_{ij}\eta_{ij} + \frac{C_{ijk\ell}}{2} \eta_{ij}\eta_{k\ell}$$

$$+ \frac{C_{ijk\ell mn}}{3!} \eta_{ij}\eta_{k\ell}\eta_{mn} + \cdots \qquad (4)$$

(Summing over repeated indices is implied.) The first two terms vanish since ϕ_0 is the energy of the unstrained medium and $\phi_1 = C_{ij}\eta_{ij}$ corresponds to displacement without deformation. Therefore, the expression for the strain energy becomes

$$\phi = \frac{C_{ijkl}}{2} \eta_{ij}\eta_{kl} + \frac{C_{ijklmn}}{3!} \eta_{ij}\eta_{kl}\eta_{mn} + \cdots \qquad (5)$$

where the strains are to be evaluated with coordinates along the propagation direction, the C_{ijkl} are the second-order elastic (SOE) constants and the C_{ijklmn} are the third-order elastic (TOE) constants (Brugger, 1964).

The SOE constants form a fourth rank tensor containing 81 components, of which 21 are independent for the most unsymmetrical triclinic crystal and the TOE constants form a sixth rank tensor with 729 components of which 56 are independent for the triclinic crystal. The number of elastic constants greatly decreases for crystals of higher symmetry. For the class of trigonal crystals under consideration there are 6 SOE and 14 TOE constants.

The equations of motion in Lagrangian coordinates are written as (Philip, 1983; Thurston and Brugger, 1964)

$$\frac{\partial T_{ij}}{\partial a_j} = \rho_0 \ddot{u}_i \qquad (6)$$

where ρ_0 is the undeformed mass density.

The equation of motion takes the following form along the a, b, and c axes of the crystal:

$$\rho_0 \ddot{u} = \frac{\partial T_{11}}{\partial a} + \frac{\partial T_{12}}{\partial b} + \frac{\partial T_{13}}{\partial c}$$

$$\rho_0 \ddot{v} = \frac{\partial T_{21}}{\partial a} + \frac{\partial T_{22}}{\partial b} + \frac{\partial T_{23}}{\partial c} \qquad (7)$$

$$\rho_0 \ddot{w} = \frac{\partial T_{31}}{\partial a} + \frac{\partial T_{32}}{\partial b} + \frac{\partial T_{33}}{\partial c}$$

The stress matrix T can be written as

$$
\begin{vmatrix} T_{11} & T_{12} & T_{13} \\ T_{21} & T_{22} & T_{23} \\ T_{31} & T_{32} & T_{33} \end{vmatrix} = \begin{vmatrix} J_{11} & J_{12} & J_{13} \\ J_{21} & J_{22} & J_{23} \\ J_{31} & J_{32} & J_{33} \end{vmatrix} \begin{vmatrix} \dfrac{\partial \phi}{\partial n_{11}} & \dfrac{\partial \phi}{\partial n_{12}} & \dfrac{\partial \phi}{\partial n_{13}} \\ \dfrac{\partial \phi}{\partial n_{21}} & \dfrac{\partial \phi}{\partial n_{22}} & \dfrac{\partial \phi}{\partial n_{23}} \\ \dfrac{\partial \phi}{\partial n_{31}} & \dfrac{\partial \phi}{\partial n_{32}} & \dfrac{\partial \phi}{\partial n_{33}} \end{vmatrix} . \tag{8}
$$

Note that the T_{ij} tensor defined here is not symmetric. Consider the case of plane finite amplitude waves propagating along the three axes of the medium under consideration. For plane waves propagating along the a axis, the displacement component becomes

$$
\begin{aligned}
u &= u(a,\, t) \\
v &= v(a,\, t) \\
w &= w(a,\, t)
\end{aligned} \tag{9}
$$

and the equations of motion for this case become

$$
\rho_0 \ddot{u} = \frac{\partial T_{11}}{\partial a} \qquad \text{(longitudinal wave)}
$$

$$
\rho_0 \ddot{v} = \frac{\partial T_{21}}{\partial a} \qquad \text{(transverse wave)} \tag{10}
$$

$$
\rho_0 \ddot{w} = \frac{\partial T_{31}}{\partial a} \qquad \text{(transverse wave)} .
$$

For longitudinal plane waves propagating along the a axis $v = 0$ and $w = 0$, so that one is left with

$$
\rho_0 \ddot{u} = \frac{\partial T_{11}}{\partial a} . \tag{11}
$$

Similarly, for plane waves propagating along the b axis

$$\rho_0 \ddot{u} = \frac{\partial T_{12}}{\partial b} \qquad \text{(transverse wave)}$$

$$\rho_0 \ddot{v} = \frac{\partial T_{22}}{\partial b} \qquad \text{(longitudinal wave)} \qquad (12)$$

$$\rho_0 \ddot{w} = \frac{\partial T_{32}}{\partial b} \qquad \text{(transverse wave)}$$

For longitudinal waves along the b axis u = 0, w = 0, and we are left with

$$\rho_0 \ddot{v} = \frac{\partial T_{22}}{\partial b} \; . \qquad (13)$$

For plane waves propagating along the c axis

$$\rho_0 \ddot{u} = \frac{\partial T_{13}}{\partial c} \qquad \text{(transverse wave)}$$

$$\rho_0 \ddot{v} = \frac{\partial T_{23}}{\partial c} \qquad \text{(transverse wave)} \qquad (14)$$

$$\rho_0 \ddot{w} = \frac{\partial T_{33}}{\partial c} \qquad \text{(longitudinal wave)} \; .$$

For longitudinal waves propagating along the c axis u = 0, v = 0 and we are left with

$$\rho_0 \ddot{w} = \frac{\partial T_{33}}{\partial c} \; . \qquad (15)$$

These equations are solved for crystals belonging to the trigonal class in the next section.

B. SECOND HARMONIC GENERATION OF ULTRASOUND
IN CRYSTALS OF TRIGONAL SYMMETRY

There are two classes of trigonal crystals (Philip, 1983), one with Hermann-Mauguin symmetry symbol $3\bar{3}$ and the other with symbol 32, 3m, $\bar{3}$m. The first class has seven SOE constants and twenty TOE constants and the latter has six SOE and fourteen TOE constants. Since the crystals of interest in this investigation, quartz and lithium niobate, belong to this class, the class 32, 3m, $\bar{3}$m is considered exclusively.

The unit cell of a crystal with trigonal symmetry is shown in Figure II-1. A rotation of the coordinate system by 120° about the [001] axis leads to an equivalent coordinate system. In the linear approximation, pure mode longitudinal waves can propagate along the x and z directions. It is a quasilongitudinal wave which propagates along the y direction since the longitudinal mode is coupled to one of the transverse modes. The elastic strain energy for the trigonal case* is (Kaga, 1968):

$$\Delta\phi(\eta) = \phi(\eta) - \phi(0) = \phi_2 + \phi_3 + \dots = \tfrac{1}{2}C_{11}(\eta_{11}^2 + \eta_{22}^2) + C_{12}\eta_{11}\eta_{22}$$

$$+ C_{13}(\eta_{22}\eta_{33} + \eta_{33}\eta_{11}) + C_{14}\{(\eta_{11} - \eta_{22})(\eta_{23} + \eta_{32}) + (\eta_{31} + \eta_{13})$$

$$(\eta_{12} + \eta_{21})\} + \tfrac{1}{2}C_{33}\eta_{33}^2$$

$$+ C_{44}(\eta_{23}^2 + \eta_{32}^2 + \eta_{31}^2 + \eta_{13}^2) + \tfrac{1}{2}(C_{11} - C_{12})(\eta_{12}^2 + \eta_{21}^2)$$

---

*The elastic constants are expressed in terms of a contracted notation (Voigt, 1928) in which 11 → 1, 22 → 2, 33 → 3, 23 → 4, 13 → 5, and 12 → 6. This means that the SOE constants have two subscripts and the TOE constants have three.

Z [001]
C-AXIS

X [100]

TRIGONAL STRUCTURE

(a)

Y [010]

Co-ordinate
Frame

c

β

α

a

γ

b

(b)

For trigonal,

$a = b = c$

$\alpha = \beta = \gamma < 120°, \neq 90°$

y [010]

b-axis

120°

x [100]

a-axis

(c) Set of equivalent
directions in a
trigonal system
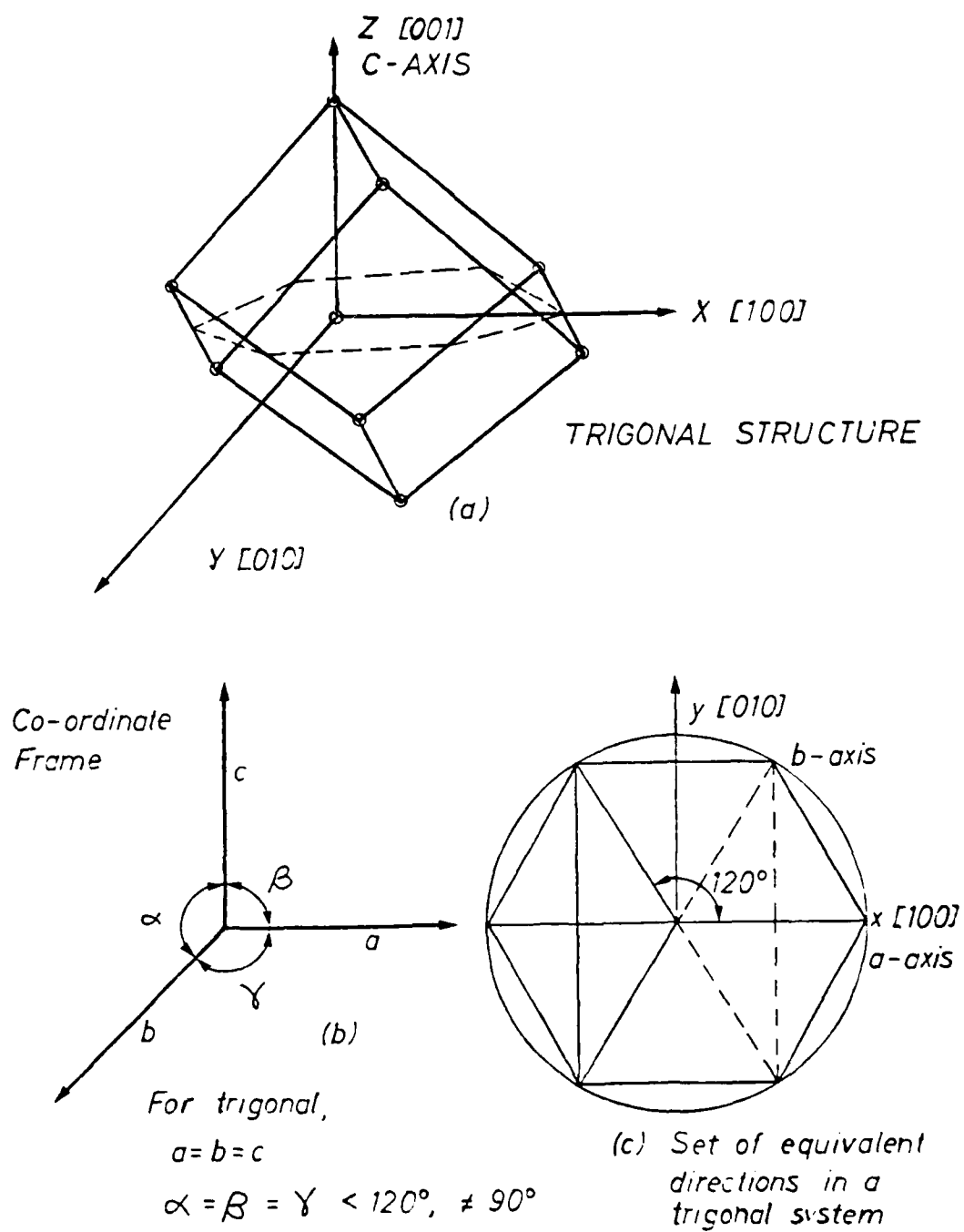
Figure II-1.   The coordinate system for crystals of trigonal symmetry.

$$+ \frac{1}{6}C_{111}\eta_{11}^3 + \frac{1}{2}C_{112}\eta_{11}^2\eta_{22} + \frac{1}{2}C_{113}(\eta_{11}^2\eta_{33} + \eta_{22}^2\eta_{11})$$

$$+ \frac{1}{2}C_{114}\eta_{11}^2(\eta_{23} + \eta_{32}) + C_{123}\eta_{11}\eta_{22}\eta_{33} + C_{124}\{\eta_{11}\eta_{22}(\eta_{23} + \eta_{32})$$

$$+ (\eta_{23} + \eta_{32})(\eta_{12}^2 + \eta_{21}^2)$$

$$+ \frac{1}{2}C_{133}\eta_{33}^2(\eta_{11} + \eta_{22}) + C_{134}\eta_{33}\{(\eta_{11} - \eta_{22})(\eta_{23} + \eta_{32})$$

$$+ (\eta_{31} + \eta_{13})(\eta_{12} + \eta_{21})\} + C_{144}\{\eta_{23}^2 + \eta_{32}^2)$$

$$+ \eta_{22}(\eta_{31}^2 + \eta_{13}^2) + C_{155}\{\eta_{22}(\eta_{23}^2 + \eta_{32}^2) + \eta_{11}(\eta_{31}^2 + \eta_{13}^2)\}$$

$$+ \frac{1}{6}C_{222}\eta_{22}^3 + \frac{1}{6}C_{333}\eta_{33}^3 + C_{344}\eta_{33}(\eta_{23}^2 + \eta_{32}^2)$$

$$+ (\eta_{31}^2 + \eta_{13}^2)\} + C_{444}\{\frac{1}{6}(\eta_{23} + \eta_{32})^3 - (\eta_{23} + \eta_{32})(\eta_{31}^2 + \eta_{13}^2)\}$$

$$+ \frac{1}{2}(C_{111} + C_{112} - C_{222})\eta_{22}^2\eta_{11}$$

$$+ \frac{1}{2}(-C_{114} - 2C_{124})\eta_{22}^2(\eta_{23} + \eta_{32}) + \frac{1}{4}(-2C_{111} - C_{112} + 3C_{222})\eta_{11}$$

$$(\eta_{12}^2 + \eta_{21}^2) + \frac{1}{4}(2C_{111} - C_{112} - C_{222})$$

$$\times \eta_{22}(\eta_{12}^2 + \eta_{21}^2) + \frac{1}{2}(C_{113} - C_{123})\eta_{33}(\eta_{12}^2 + \eta_{21}^2) + \frac{1}{2}(C_{114}$$

$$+ 3C_{124})\eta_{11}(\eta_{31} + \eta_{13})(\eta_{12} + \eta_{21})$$

$$+ \frac{1}{2}(C_{114} - C_{124})\eta_{22}(\eta_{31} + \eta_{13})(\eta_{12} + \eta_{21}) + \frac{1}{2}(-C_{144} + C_{155})$$

$$(\eta_{23} + \eta_{32})(\eta_{31} + \eta_{13})(\eta_{12} + \eta_{21}) + \dots \tag{16}$$

The strain derivatives were calculated (Philip, 1983) and from those derivatives the components of the stress tensor were obtained. From that point the equations of motion were found for pure mode

longitudinal waves propagating along the symmetry directions [100] and [001] which are, respectively, the a and c axes.

It is found that the equation of motion has the same form in each case

$$\rho_0 \ddot{u} - \alpha u_{aa} = \zeta u_a u_{aa} \qquad (17)$$

with different values for the α and ζ for different directions. This equation shows that pure mode longitudinal waves propagate along these directions. The effect of the nonlinear term $\zeta u_a u_{aa}$ is to be determined.

A perturbation solution was obtained by Philip (1983) similar to the technique used for the case of cubic symmetry. Let:

$$u = u^0 + u' \qquad (18)$$

where $u' \ll u^0$ and use the trial solution

$$u^0 = A \sin(ka - \omega t) \qquad (19)$$

and

$$u' = B \ a \ \sin 2(ka - \omega t) + C \ a \ \cos 2(ka - \omega t)$$

as the perburbation term. After one iteration the solution of the equation of motion becomes

$$u(a,t) = A \sin(ka - \omega t) - \left[\frac{(kA)^2 \zeta}{8 \rho_0 C_0^2}\right] a \ \cos 2(ka - \omega t) \ . \qquad (20)$$

The equation of motion also can be written as

$$\rho_0 \frac{\partial^2 u}{\partial t^2} - \alpha \frac{\partial^2 u}{\partial a^2} = \zeta \frac{\partial u}{\partial a} \frac{\partial^2 u}{\partial a^2} . \tag{21}$$

Breazeale and Ford (1965) arrived at the same equation from the fluid analogy of cubic crystals but divided the nonlinear terms as follows:

$$\rho_0 \frac{\partial^2 u}{\partial t^2} = K_2 \left(\frac{\partial^2 u}{\partial a^2} + 3 \frac{\partial u}{\partial a} \frac{\partial^2 u}{\partial a^2} \right) + K_3 \frac{\partial u}{\partial a} \frac{\partial u^2}{\partial a^2} \tag{22}$$

or

$$\rho_0 \frac{\partial^2 u}{\partial t^2} - K_2 \frac{\partial^2 u}{\partial a^2} = (3K_2 + K_3) \frac{\partial u}{\partial a} \frac{\partial^2 u}{\partial a^2} . \tag{23}$$

The equations are the same if $\alpha = K_2$ and

$$\zeta = (3K_2 + K_3) . \tag{24}$$

Now consider the linear part of the wave equation

$$\rho_0 \frac{\partial^2 u}{\partial t^2} = \alpha \frac{\partial^2 u}{\partial a^2} \tag{25}$$

$$\frac{\partial^2 u}{\partial t^2} = \left(\frac{\alpha}{\rho_0} \right) \frac{\partial^2 u}{\partial a^2} . \tag{26}$$

Comparing with the wave equation

$$\frac{\partial^2 u}{\partial t^2} = C_0^2 \frac{\partial^2 u}{\partial a^2} \tag{27}$$

where C_0 is the phase velocity, and

$$C_0^2 = \frac{\alpha}{\rho_0}$$

$$\alpha = \rho_0 \, C_0^2 \tag{28}$$

$$K_2 = \alpha = \rho_0 \, C_0^2 \;.$$

Thus the solution to the wave equation for trigonal symmetry can be written

$$u(a,t) = A \sin(ka - \omega t) - [\frac{(3K_2 + K_3)}{8K_2}](kA)^2 a \cos 2(ka - \omega t). \tag{29}$$

as long as K_2 and K_3 previously defined for cubic symmetry are interpreted in terms of trigonal symmetry.

As in the case of cubic crystals, we can define the ultrasonic nonlinearity parameter for trigonal crystals as the negative of the ratio of the nonlinear term to the linear term in the wave equation. Thus the nonlinearity parameter is

$$\beta = -\frac{3K_2 + K_3}{K_2} \;. \tag{30}$$

For an initially sinusoidal disturbance at $a = 0$ the solution to the nonlinear equation can be written in terms of the nonlinearity parameter as:

$$u = A_1 \sin(ka - \omega t) + \frac{A_1^2 k^2}{8} \, \beta \cos 2(ka - \omega t) \tag{31}$$

where A_1 is the amplitude of the fundamental wave and

$$A_2 = \frac{A_1^2 k^2 a \beta}{8} \tag{32}$$

is the amplitude of the generated second harmonic. In terms of A_2 and A_1, β is given by

$$\beta = 8 \frac{A_2}{A_1^2} \frac{1}{k^2 a} \;, \tag{33}$$

or,

$$K_3 = -K_2(3 + \beta) \ . \tag{34}$$

Therefore, by measuring the fundamental amplitude A_1 and the second harmonic amplitude A_2, one can determine   which can then be used to evaluate K_3, the linear combination of TOE constants. The parameters K_2 and K_3 are given for each symmetry direction considered for trigonal crystals in Table II-1.

TABLE II-1

THE K_2 AND K_3 PARAMETERS FOR TRIGONAL SYMMETRY

Direction of Wave Propagation	K_2	K_3
[100]	C_{11}	C_{111}
[001]	C_{33}	C_{333}

C. SECOND HARMONIC GENERATION IN TRIGONAL PIEZOELECTRIC CRYSTALS

The Nonpiezoelectric Case

The equation of motion

$$\rho_0 \ddot{u}_i = \frac{\partial T_{ik}}{\partial a_k} \tag{35}$$

also can be written

$$\rho_0 \ddot{u}_i = \frac{\partial}{\partial a_k} \left[\frac{\partial x_i}{\partial a_m} \frac{\partial \phi}{\partial \eta_{km}} \right] \tag{36}$$

(McMahon, 1968) where the strain energy

$$\phi = \frac{C_{ijk\ell}}{2} n_{ij}n_{i\ell\ell} + \frac{C_{ijk\ell mn}}{3!} n_{ij}n_{k\ell}n_{mn} + \cdots .$$ (37)

It is convenient to follow Thurston (1964), who defines the thermo-dynamic tension

$$t_{km} = \frac{\partial \phi}{\partial n_{km}}$$ (38)

so that the equation of motion becomes

$$\rho_0 \ddot{u}_i = \frac{\partial}{\partial a_k} \left[\frac{\partial x_i}{\partial a_m} t_{km} \right] .$$ (39)

The analysis which follows is made in terms of t_{km}.

Piezoelectric Solids

Now, consider a piezoelectric solid. McMahon (1968) points out that if one holds the electric field constant, the strains resulting from an acoustical disturbance directly produce stresses by means of the elastic constants. If the electric field is free to vary, the same result is produced by an indirect process. The applied strain produces a polarization (direct piezoelectric effect) and consequently an electric field is produced by means of the electric susceptibility. This electric field in turn (increased piezoelectric effect) produces a stress. Therefore as a consequence of the piezoelectric coupling, oscillating strain fields are accompanied by oscillating electric fields. These oscillating electric fields contribute to the terms in the internal energy expression and thus produce changes in both SOE constants and the TOE constants. The overall effect of

the piezoelectric coupling is that the second-, third- and higher-order elastic constants are not equal to the elastic constants measured at constant applied electric fields. The constants then are said to have been "stiffened" by piezoelectric coupling.

In a piezoelectric solid the internal energy is a function of the entropy, strain and electric displacement. In order to have as variables the entropy, strain and electric field, one introduces the thermodynamic potential H_2 which is the electric enthalpy. One defines the enthalpy H_2 as the difference $\phi - E_i D_i$, where ϕ is the internal energy per unit undeformed volume, E_i the electric field, and D_i the electric displacement (Dieulesaint and Royer, 1980; Graham, 1977; Baryshnikova and Lyamov, 1978). Expanding the enthalpy to include the elastic, electric, piezoelectric and higher-order terms:

$$H_2 = \frac{1}{2} C^{(E)}_{ijk\ell} \eta_{ij}\eta_{k\ell} + \frac{1}{6} C^{(E)}_{ijk\ell mn} \eta_{ij}\eta_{k\ell}\eta_{mn}$$

$$- \frac{1}{2} \epsilon^{(S)}_{ij} E_i E_j - \frac{1}{6} \epsilon^{(S)}_{ijk} E_i E_j E_k - e_{ijk} E_i \eta_{jk} - \frac{1}{2} d_{ijk\ell} E_i E_j \eta_{k\ell}$$

$$- \frac{1}{2} f_{ijk\ell m} E_i \eta_{jk} \eta_{\ell m} \tag{40}$$

where η_{ij} are the strain components and E_i are the electric field components. The superscripts E and S indicate measurement, respectively, at constant applied electric field and constant strain. The material constant e_{ijk} is the piezoelectric coupling constant. The constants $d_{ijk\ell}$ and $f_{ijk\ell m}$ are higher-order cross term coefficients. The physical basis of each coefficient is as follows: $\epsilon^{(S)}_{ijk}$ is related to the nonlinear optic and electrooptic effects; $d_{ijk\ell}$ is related both

to elastooptic and electrostrictive effects; and $f_{ijk\ell m}$ is related to the electroacoustic effect (change in velocity of sound with applied electric field). The lack of magnitudes of the $f_{ijk\ell m}$ has prevented evaluation of the constant electric field TOE constants. It should be noted that the material constants in the above expression are functions of the relative frequency of the strain and electric field components. If both the electric field and strain frequencies lie in the ultrasonic frequency range, then the value of these constants is not necessarily equal to either their static value or to their value at optical frequencies.

The correlation of the magnitude of the oscillating electric field with the amplitude of the accompanying ultrasonic wave, is given by[*] (Baryshnikova and Lyamov, 1978).

$$t_{ij} = \frac{\partial H_2}{\partial \eta_{ij}} \tag{41}$$

$$D_i = -\frac{\partial H_2}{\partial E_i} \tag{42}$$

Therefore:

---

*Note that throughout this development contracted notation (Voigt, 1928) of the indices is not used until the relationships are developed then contracted notation is used when later on an actual numerical substitution is made into the relationship.

$$t_{ij} = c^{(E)}_{ijk\ell}\eta_{k\ell} + \frac{1}{2} c^{(E)}_{ijk\ell mn}\eta_{k\ell}\eta_{mn} - e_{kij}E_k - \frac{1}{2} d_{k\ell ij}E_kE_\ell$$

$$- f_{mijk\ell}E_m\eta_{k\ell} \tag{43}$$

$$D_i = \epsilon^{(S)}_{ij}E_j + e_{ijk}\eta_{jk} + \frac{1}{2}\epsilon^{(S)}_{ijk}E_jE_k + d_{ijk\ell}E_j\eta_{k\ell}$$

$$+ \frac{1}{2} f_{ijk\ell m}\eta_{jk}\eta_{\ell m} \cdot \tag{44}$$

In addition, a solution to the coupled electromagnetic-elastic wave problem uses the wave equation derived from Maxwell's equations:

$$\nabla^2 E_i = \mu \ddot{D}_i , \tag{45}$$

solves it simultaneously with the nonlinear elastic equation of motion:

$$\rho_0 \ddot{u} = \frac{\partial}{\partial a_k} \left[\frac{\partial x_i}{\partial a_m} t_{km} \right] , \tag{46}$$

and seeks a solution for plane waves propagating along the a_1 crystal direction. The material constants in the expansion of the enthalpy are then expressed in terms of the orthogonal Cartesian coordinate system by means of a tensor transformation for rotated axes. In this rotated coordinate frame, one can write the three component equations from Eq. (45) as:

$$(\vec{\nabla} \times \vec{H})_1 = \dot{D}_1 = 0 \tag{47}$$

$$\frac{\partial^2 E_p}{\partial a_1^2} = \mu \ddot{D}_p \quad p \neq 1 \tag{48}$$

In order to get a solution one expands the electric field in a power series of strain

$$E_i = \alpha_{i1k}n_{1k} + \beta_{i1k1m}n_{1k}n_{1m} \cdot \tag{49}$$

The values of the α's and β's are determined by substituting (49) into Maxwell's equations. If one substitutes (44) into (47) and eliminates E_i through (49), one gets the result

$$0 = \dot{D}_1 = (\varepsilon_{1j}^{(S)}\alpha_{j1k} + e_{11k})\dot{n}_{1k} + 2(\varepsilon_{1j}^{(S)}\beta_{j1\ell 1m} + d_{1j1\ell}\alpha_{j1m}$$

$$+ \frac{1}{2}\varepsilon_{1jk}^{(S)}\alpha_{j1\ell}\alpha_{k1m} + \frac{1}{2}f_{11\ell 1m})n_{1\ell}\dot{n}_{\ell m}$$

$$+ \text{ higher order products of strain and strain}$$
$$\text{derivatives.} \tag{50}$$

Since n_{ij} is an arbitrary function of time, the first-, second- and higher-order coefficients must separately vanish. Therefore, one obtains the following relationships:

$$\varepsilon_{1j}\alpha_{j1k} + e_{11k} = 0 \tag{51}$$

$$\varepsilon_{1j}^{(S)}\beta_{j1\ell 1m} + d_{1j1\ell}\alpha_{j1m} + \frac{1}{2}\varepsilon_{1jk}^{(S)}\alpha_{j1\ell}\alpha_{k1m} + (\frac{1}{2})f_{11\ell 1m} = 0 \ . \tag{52}$$

In order to eliminate the time and spatial differentials from Eq. (45) one assumes a plane wave solution for the electric field and displacements of the form:

$$E_i = E_i(1)e^{i(ka_1 - \Omega t)} + E_i(2)e^{2i(ka_1 - \Omega t)} + \dots$$

$$u_i = u_i(1)e^{i(ka_1 - \Omega t)} + u_i(2)e^{2i(ka_1 - \Omega t)} + \dots \; . \tag{53}$$

The condition that the exchange of energy take place between the acoustic and electric waves and their respective harmonics proceeds sufficiently slowly so that the amplitude change is small in one wavelength of sound and can be written as:

$$\frac{\partial u_i(1)}{\partial a_1} \ll iku_i(1) \tag{54}$$

$$\frac{\partial E_i(1)}{\partial a_1} \ll ikE_i(1) \; . \tag{55}$$

This condition is almost always met in practice, so if one neglects the slow change in amplitude, then the spatial and time derivatives are proportional to one another. This can be expressed as:

$$\frac{\partial}{\partial a_1} = -\left(\frac{k}{\Omega}\right)\frac{\partial}{\partial t} \; . \tag{56}$$

If this relationship is satisfied, Maxwell's equation for the transverse electric-field components can be integrated immediately with the result

$$\epsilon E_p = D_p \; , \tag{57}$$

where we have defined

$$\epsilon \equiv \frac{1}{u}\left(\frac{k}{\Omega}\right)^2 .$$

(58)

By substituting Eqs. (44) and (49) into Eq. (57), Eq. (57) can be written as

$$\epsilon(\alpha_{plk}\eta_{lk} + \beta_{pklm}\eta_{lk}\eta_{lm}) = (\epsilon_{pj}^{(S)}\alpha_{jlk} + e_{plk})s_{lk}$$

$$+ (\epsilon_{pj}\beta_{jlklm} + d_{pjlk}\alpha_{jlm} + \frac{1}{2}\epsilon_{pij}^{(S)}\alpha_{ilk}\alpha_{jlm}$$

$$+ \frac{1}{2}f_{plklm})\eta_{lk}\eta_{lm} .$$

(59)

Because the strain components are arbitrary functions of time the linear and quadratic terms are separately equal to each other. This gives the remaining relationships necessary for the determination of the α's and β's:

$$\epsilon\alpha_{plk} = \epsilon_{pj}^{(S)}\alpha_{jlk} + e_{pik}$$

(60)

$$\epsilon\beta_{plklm} = \epsilon_{pj}^{(S)}\beta_{jlklm} + d_{pjlk}\alpha_{jlm}$$

$$+ \frac{1}{2}\epsilon_{pij}^{(S)}\alpha_{ilk}\alpha_{jlm} + \frac{1}{2}f_{plklm} .$$

(61)

When the second order terms are retained in the enthalpy, the solution of five simultaneous equations [(46) and (48)] consists of five normal modes representing the quasitransverse electromagnetic waves. The presence of piezoelectric coupling therefore only slightly

affects the characteristics of the acoustical and electromagnetic wave. Adding higher-order terms to the enthalpy still does not affect the resolution into quasielastic and quasielectromagnetic waves. Therefore if one considers only the quasiacoustic wave motion and one represents the velocity of light and the velocity of sound in the medium by the respective symbols c and v, one can write

$$u\varepsilon = (\frac{k}{\omega})^2 = \frac{1}{v^2} \, , \tag{62}$$

whereas $u\varepsilon_{ij}^{(S)} \approx \frac{1}{2} \ll u\varepsilon$. Since the first term on the right-hand sides of Eqs. (60) and (61) are smaller by a factor of $(v/c)^2$ than the respective terms on the left-hand sides of the equations, one can with little error simplify these equations to read:

$$\alpha_{plk} = e_{plk}/\varepsilon \tag{63}$$

$$\varepsilon\beta_{plklm} = d_{pilk}\alpha_{ilm} + (\frac{1}{2})\varepsilon_{pij}^{(S)}\alpha_{i\ell k}\alpha_{j\ell m} + \frac{1}{2} f_{plklm} \, . \tag{64}$$

Comparing Eq. (51) with Eq. (63) shows that

$$\alpha_{plk} \ll |\alpha_{11k}| \, , \tag{65}$$

which can be used to obtain the following values for the coefficients:

$$\alpha_{11k} = -\frac{e_{11k}}{\varepsilon_{11}^{(S)}} \, , \quad \alpha_{plk} = 0 \, . \tag{66}$$

A comparison of Eq. (64) and Eq. (52) similarly shows

$$\beta_{plklm} \ll \beta_{11klm} .$$ (67)

Equation (52) can be solved to give

$$\epsilon_{11}^{(S)}\beta_{11klm} = -d_{111k}\alpha_{11m} - (\tfrac{1}{2})\epsilon_{111}^{(S)}\alpha_{11k}\alpha_{11m} - \tfrac{1}{2}f_{11klm} .$$ (68)

From Eq. (67) one can assume

$$\beta_{plklm} = 0 .$$ (69)

Comparison of the relative sizes of the coefficients α_{jlk} and β_{jlklm} shows that E_2 and E_3 are smaller than E_1 by the ratio $(v/c)^2$. Consequently, one makes the approximation $E_2 = E_3 = 0$. The value for E_1 then is found by substituting Eqs. (66) and (68) into Eq. (49). The result of the substitution is

$$E_1 = -\frac{e_{11k}}{\epsilon_{11}^{(S)}}\eta_{1k} + [\frac{d_{111k}e_{11\ell}}{\epsilon_{11}^{(S)}} - \frac{1}{2}\frac{\epsilon_{111}^{(S)}e_{11k}e_{11\ell}}{(\epsilon_{11}^{(S)})^3}$$
$$- \frac{1}{2\epsilon_{11}^{(S)}}f_{11k1\ell}]\eta_{1k}\eta_{1\ell} .$$ (70)

The next step is to substitute the value of E_1 into the expression for t_{ij}. For elastic waves traveling along the a_1 axis, t_i, defined by Eq. (41), is

$$t_{ij} = C_{ij1\ell}^{(E)}\eta_{1\ell} - e_{1ij}E_1 - (\tfrac{1}{2})d_{11ij}E_1^2 - f_{1ij1\ell}E_1\eta_{1\ell}$$
$$+ \frac{1}{2}C_{ij1\ell1m}^{(E)}\eta_{1\ell}\eta_{1m} .$$ (71)

If E_1 is eliminated using Eq. (70)

$$t_{ij} = [C_{ijlk}^{(E)} + \frac{e_{11k}e_{1ij}}{\varepsilon_{11}^{(S)}}]\eta_{1k} + \frac{1}{2}\eta_{1k}\eta_{1\ell}[C_{ijik1\ell}^{(E)} + \frac{\varepsilon_{111}^{(S)}e_{11k}e_{11\ell}e_{1ij}}{(\varepsilon_{11}^{(S)})^3}$$

$$+ \frac{f_{11\ell1k}e_{1ij}}{\varepsilon_{11}^{(S)}} + \frac{2f_{1ij1\ell}e_{11k}}{\varepsilon_{11}^{(S)}} - \frac{2e_{11\ell}e_{1ij}d_{111k}}{(\varepsilon_{11}^{(S)})}$$

$$- \frac{e_{11\ell}e_{11m}d_{11ij}}{(\varepsilon_{11}^{(S)})^2}] . \tag{72}$$

Comparison with the nonpiezoelectric expression derived from substituting ϕ into $t_{km} = \frac{\partial\phi}{\partial\eta_{km}}$, gives the following result:

$$C_{ijlk} = C_{ijlk}^{(E)} + e_{11k}\,e_{1jk}/\varepsilon_{11}^{(S)} \tag{73}$$

$$C_{ijlklm} = C_{ijlklm}^{(E)} + \frac{\varepsilon_{111}^{(S)}e_{11k}e_{11m}e_{1ij}}{(\varepsilon_{11}^{(S)})^3} + \frac{e_{1ij}f_{11klm}}{\varepsilon_{11}^{(S)}}$$

$$+ \frac{2e_{11k}f_{1ij1m}}{\varepsilon_{11}^{(S)}} - \frac{2e_{11k}e_{1ij}d_{111m}}{\varepsilon_{11}^{(S)}} - \frac{e_{11k}e_{11m}d_{11ij}}{(\varepsilon_{11}^{(S)})^2} \tag{74}$$

The only change that is made necessary by the use of piezoelectric crystals, then, is that the elastic constants are replaced by the effective elastic constants given above.

Now, consider elastic longitudinal waves traveling along the (piezoelectric) Z axis of LiNbO$_3$. Using the condensed Voigt notation one gets

$$C_{33} = C_{33}^{(E)} + [(e_{33})^2/\varepsilon_{33}^{(S)}] \tag{75}$$

$$C_{333} = C_{333}^{(E)} + \varepsilon_{333}^{(S)}(e_{33}/\varepsilon_{22}^{(S)})^3 + \frac{3f_{333}e_{33}}{\varepsilon_{33}^{(S)}} - e_{333}^2 d_{333}(\frac{2}{\varepsilon_{33}^{(S)}}) + \frac{1}{\varepsilon_{33}^{(S)^2}})$$

(76)

This expression differs from McMahon's Eq. (34) in the final term. The conclusion is not affected by this difference. (Mathur and Gupta (1970) repeat McMahon's expression even though they carry the calculation to the next higher order term.) The conclusion is that the effective nonlinearity parameter may be written (McMahon, 1968; Zarembo and Krasilnikov, 1971; Carr, 1968) as:

$$\beta = \frac{8A_2}{A_1^2 k^2 a} = -(\frac{3C_{33} + C_{333}}{C_{33}})$$

(77)

or,

$$C_{333} = -C_{33}(3 + \beta) .$$

(78)

It would be desirable to isolate C_{333}^E; however, to date this has been prevented for lack of experimental values of f_{333}. Since the X-direction in LiNbO$_3$ is not a piezoelectric direction for a longitudinal wave, it is not necessary to make these considerations with respect to the magnitude of C_{111}. In quartz these considerations with respect to C_{333} are not necessary because the Z-direction is not a piezoelectric direction for longitudinal waves. For quartz the X-direction is a piezoelectric direction for longitudinal waves; however, the difference between C_{111} and C_{111}^E is smaller than experimental uncertainty (Thurston et al., 1966).

CHAPTER III

EXPERIMENTAL APPARATUS AND PROCEDURE

The ultrasonic nonlinearity parameter β is determined by measuring the amplitudes of both the fundamental and second harmonic of a longitudinal wave propagating in a pure mode direction in a solid. Let A_1 correspond to the fundamental amplitude and A_2 correspond to the amplitude of the second harmonic. In the theory of finite wave propagation, A_2 is proportional to A_1^2 in the limit of infinitesimal fundamental amplitude (Thurston and Shapiro, 1967) or equivalently for an infinite discontinuity distance (Breazeale and Ford, 1965). Therefore, measurements were made using the smallest fundamental amplitude which provided a workable signal-to-noise ratio for the second harmonic, and an extrapolation to zero amplitude was made.

The frequency of the fundamental signal was chosen to be 30 MHz as a compromise between two opposing processes. The amplitude of the second harmonic is proportional to the square of the frequency which implies that a higher frequency leads to a better signal-to-noise ratio. On the other hand, attenuation and the effects of non-parallelism also increase with increasing frequency. Therefore, 30 MHz has been found to be the best compromise.

In making nonlinear measurements, the pulse echo technique is used in order to avoid complications arising from interference effects.

31

A. THE ROOM TEMPERATURE CAPACITIVE RECEIVER

The absolute measurements of amplitude are made using the capacitive receiver pictured in Figure III-1. A diagram of the apparatus is shown in Figure III-2. The apparatus has a detecting electrode held in place by a fused silica optical flat in such a way that it remains insulated from the outer ground ring which is the electrical ground of the system.

The detector electrode and ground ring are lapped optically flat to within 2-3 fringes of helium light. The detector electrode is centered in the ground ring and recessed to a depth of from 5-10 microns below the face of the ground ring. The sample face is also made optically flat and coated with a thin coating ($\sim$ 1000 Å) of copper by vacuum evaporation. The sample is then positioned on the ground ring so that the combination makes a parallel plate capacitor at the end of the sample with a gap spacing of from 5-10 microns. A bias voltage of approximately 150 volts is applied to the detecting electrode through a 1 megohm resistor whose purpose is to limit the current through the detector in case of arcing.

On the top surface of the sample, an X-cut quartz transducer is attached with nonaq stopcock grease. The resonant frequency of the transducer is 30 MHz. The high voltage copper electrode is electrically insulated from the rest of the apparatus by a teflon ring. It is spring-loaded to insure good contact with the transducer. When a plane longitudinal wave is incident on the sample face causing it to vibrate, the gap spacing is changed and an alternating voltage is induced between the detecting electrode and ground.
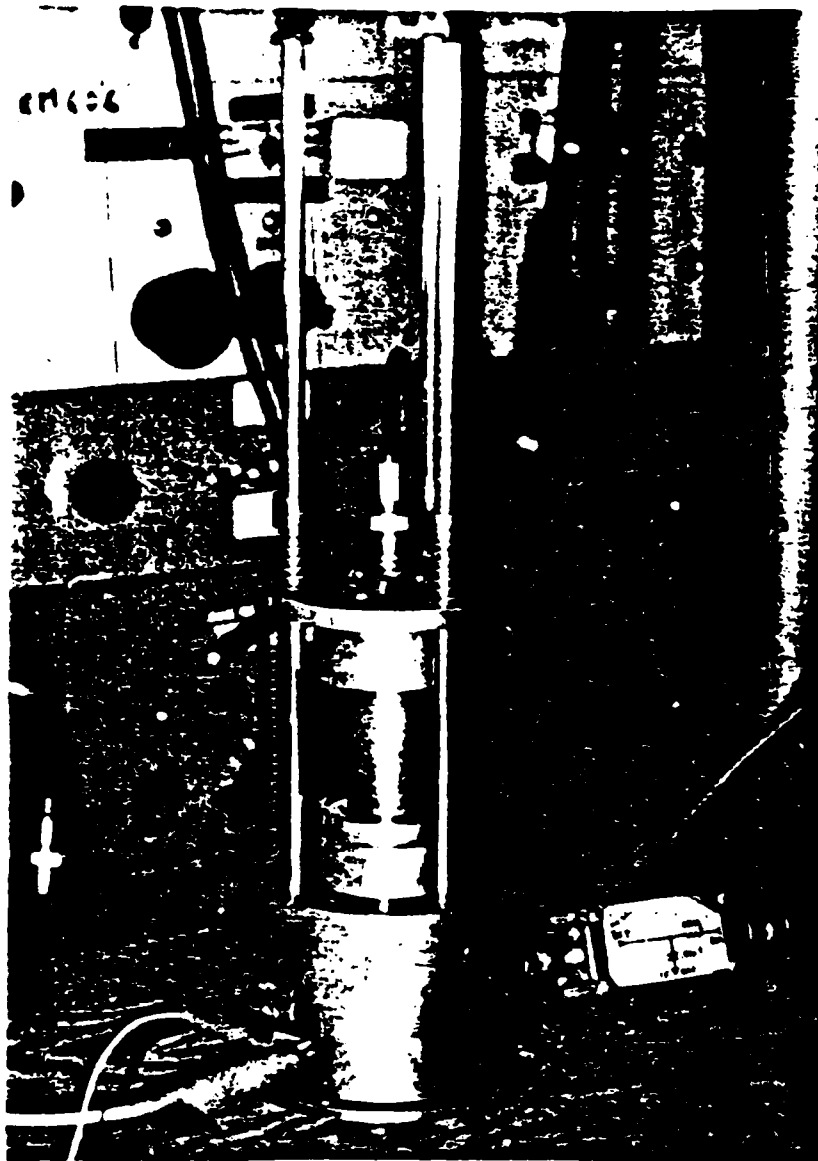
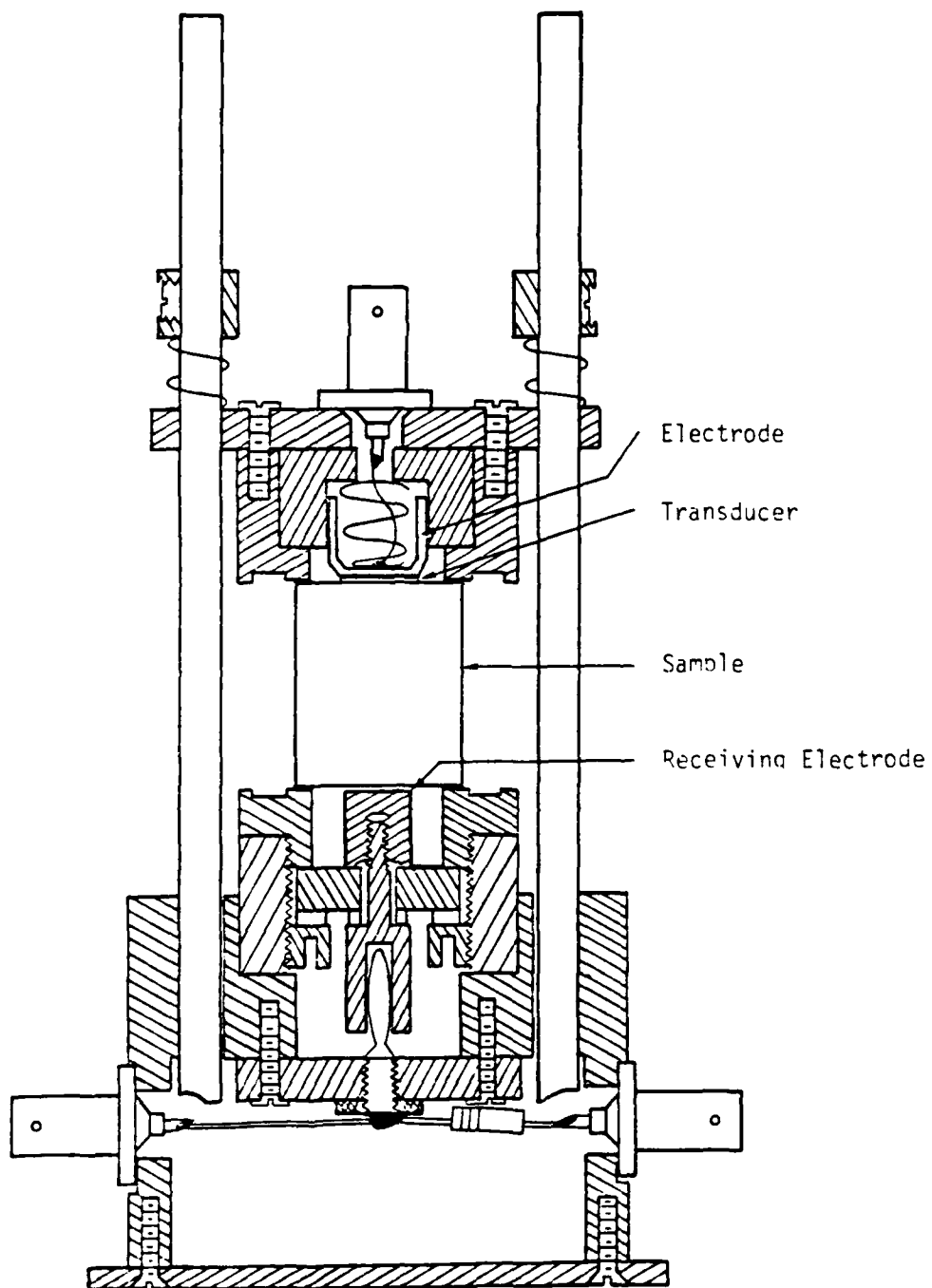Figure III-1. The capacitive detector.

Figure III-2. Cross sectional view of the detector apparatus.

B. CALIBRATION PROCEDURES

The calibration of the capacitive receiver which is required for absolute measurement of amplitude is done by the introduction of a continuous wave (c.w.) substitutional signal which replaces the acoustically generated electrical signal. An R.F. generator and an R.F. voltmeter are attached to the detector button in such a way that the capacitive detector is not removed from the circuit during calibration. The equivalent circuit of the setup is the Norton equivalent. This is represented in Figure III-3 where the parameters of that circuit are defined as follows:

C_D is the quiescent capacitance of the detector;

C_S is the stray capacitance of the detector;

L is the inductance of the wire leading from the banana jack
to the BNC connector (refer to diagram of the apparatus);

Z is the impedance of the resistor located at the base of the
apparatus;

G_D is the current generator of the Norton equivalent circuit of
the detector;

G_S is the substitutional current generator;

i_D is the amplitude of the current produced by the ultrasonic
signal;

i_S is the amplitude of the substitutional current;

S_1 is a switch that is opened and closed by turning on and off
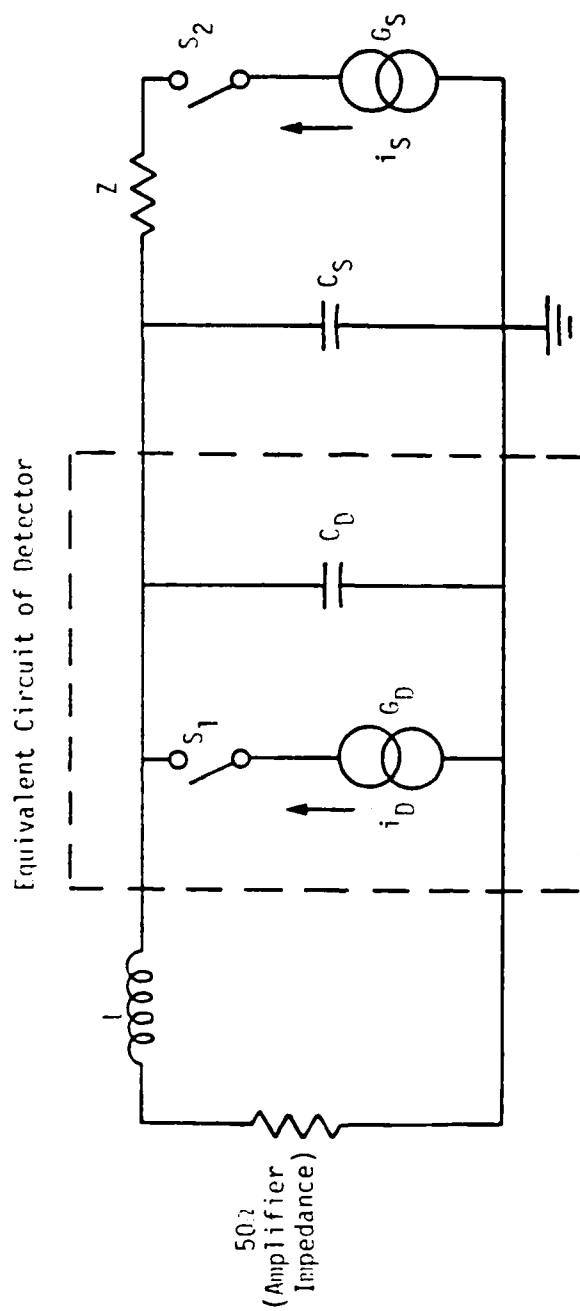the ultrasonic pulse.

Figure III-3. Equivalent circuit used for the displacement amplitude measurements.

The series combination of the inductance, the amplifier input impedance in parallel with the detector capacitance C_D and stray capacitance C_S, form the total impedance of the detector circuit. The substituional signal current i_S flows through the same impedance as the acoustical signal current i_D.

Peters (1968) showed that the Thévenin equivalent circuit of the capacitive receiver is a voltage of amplitude

$$V = \frac{2AV_b}{S_0} \tag{79}$$

where A is the amplitude of the ultrasonic wave, V_b is the bias voltage applied to the detector, and S_0 is the static gap spacing. The amplitude of vibration of the free surface of the sample is twice the amplitude within the sample because the incident and reflected waves add. This is where the factor of 2 enters into Eq. (79).

The current amplitude i_D produced by the capacitive detector is related to the voltage amplitude V by

$$i_D = V\omega C_D , \tag{80}$$

where ω is the angular frequency of the ultrasonic wave. By combining equations one gets the current generated by the detector in the Norton equivalent circuit (Bains, 1974):

$$i_D = \frac{2AV_b\omega C_D}{S_0} . \tag{81}$$

The substitutional generator $G\omega$ is adjusted to give the same output from the amplifier as with the acoustical signal. When this condition is satisfied,

$$i_D = i_S . \tag{82}$$

The current is measured by means of the voltage V_S across the current generator G_S and by measuring the impedance of the remainder of the circuit. The resulting expression for i_S is

$$i_S = \frac{V_S}{\left| Z + [j\omega(C_D + C_S) + \frac{1}{50 + j\omega L}]^{-1} \right|} . \tag{83}$$

The quantity Z is the impedance of the resistor located between the substitutional source and the capacitive detector. The resistor does not act as a pure resistance at the frequency used in this work; therefore, it is necessary to measure the impedance of the resistor at each frequency used in the measurements. The impedance measurements on R are made with a vector voltmeter. The sample detector assembly and bottom plate are removed from the apparatus and 50Ω terminators are connected to the two BNC connectors at the base. A CW variable frequency oscillator (VFO) is connected to the side having the resistor. Both vector voltmeter (Hewlett-Packard 8405A) probes with isolator tips are placed at point 1 as shown in Figure III-4 and the phase angle between the signals is zeroed and the amplitudes are measured. Probe A of the voltmeter is then left at point 1 while probe B is
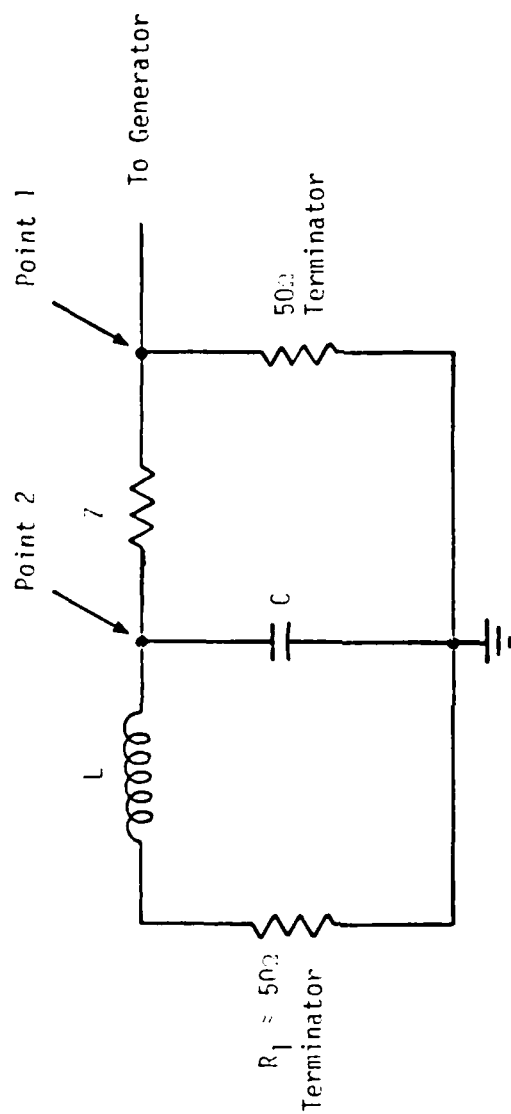
Figure III-4. Circuit used for the measurement of the impedance Z.

moved to point 2. The VFO signal generator is readjusted to obtain

the same reading of the voltmeter A channel amplitude as before and

the amplitude of the B channel and phase between the probes is

measured. This is done for both fundamental and second harmonics.

The impedance Z is calculated from

$$Z = [j\omega C + \frac{1}{R_1 + j\omega L}]^{-1} \frac{V_{B_1} - V_{B_2} e^{j\phi}}{V_{B_2} e^{j\phi}} \tag{84}$$

where C is the stray capacitance at point 2, including the probe tip;

R_1 is the resistance of the precision terminator measured with an

impedance bridge; V_{B_1} and V_{B_2} are the voltages measured by probe B

at points 1 and 2, respectively, and ϕ is the phase angle. A computer

program is used in which the Lagrange five-point interpolation

formula enables one to calculate $|Z|$ as a function of frequency in the

range 28 MHz to 32 MHz in increments of .01 MHz and from 56 MHz to

64 MHz in increments of .02 MHz. This covers the range in which

impedance measurements are required. The resistor has an impedance

of approximately 10KΩ. As a consequence, Z is much larger than the

other impedances in the apparatus and to a good approximation

Eq. (83) can be written as

$$i_s = \frac{V_s}{|Z|} . \tag{85}$$

Therefore substituting into (82) one obtains

$$A = \frac{V_S\, S_0}{2V_b\omega C_D |Z|} \qquad (86)$$

or

$$\frac{A_2}{A_1^{\,2}} = \left(\frac{V_{S_2}}{V_{S_1}^{\,2}}\right) \frac{V_b\omega_1 C_D}{S_0} \frac{|Z_1|}{|Z_2|}) \ . \qquad (87)$$

C. EXPERIMENTAL APPARATUS

A block diagram of the experimental setup used for making room temperature measurements is given in Figure III-5. A photograph of the setup appears in Figure III-6. An RF oscillator is used to drive a gated amplifier. The pulses are then passed through an impedance matching network and a 30 MHz bandpass filter to insure spectral purity of the ultrasonic wave. The pulsed signal is then used to drive the 30 MHz transducer which has been bonded to the sample with nonaq stopcock grease. The pulsed signal from the capacitive detector is then fed to either a 30 MHz or 60 MHz bandpass amplifier which rectifies the RF signal and produces an output which is the envelope of the rectified pulse. The output from the ampli-fier is monitored with an oscilloscope and the voltage level is measured with a boxcar averager. The output of the boxcar averager is proportional to the time average of the input. Therefore, random noise is averaged to zero and the repetitive signal is measurable even at levels below the noise level. This signal processing capability is particularly useful in measuring the extremely low level signals from the second harmonic.
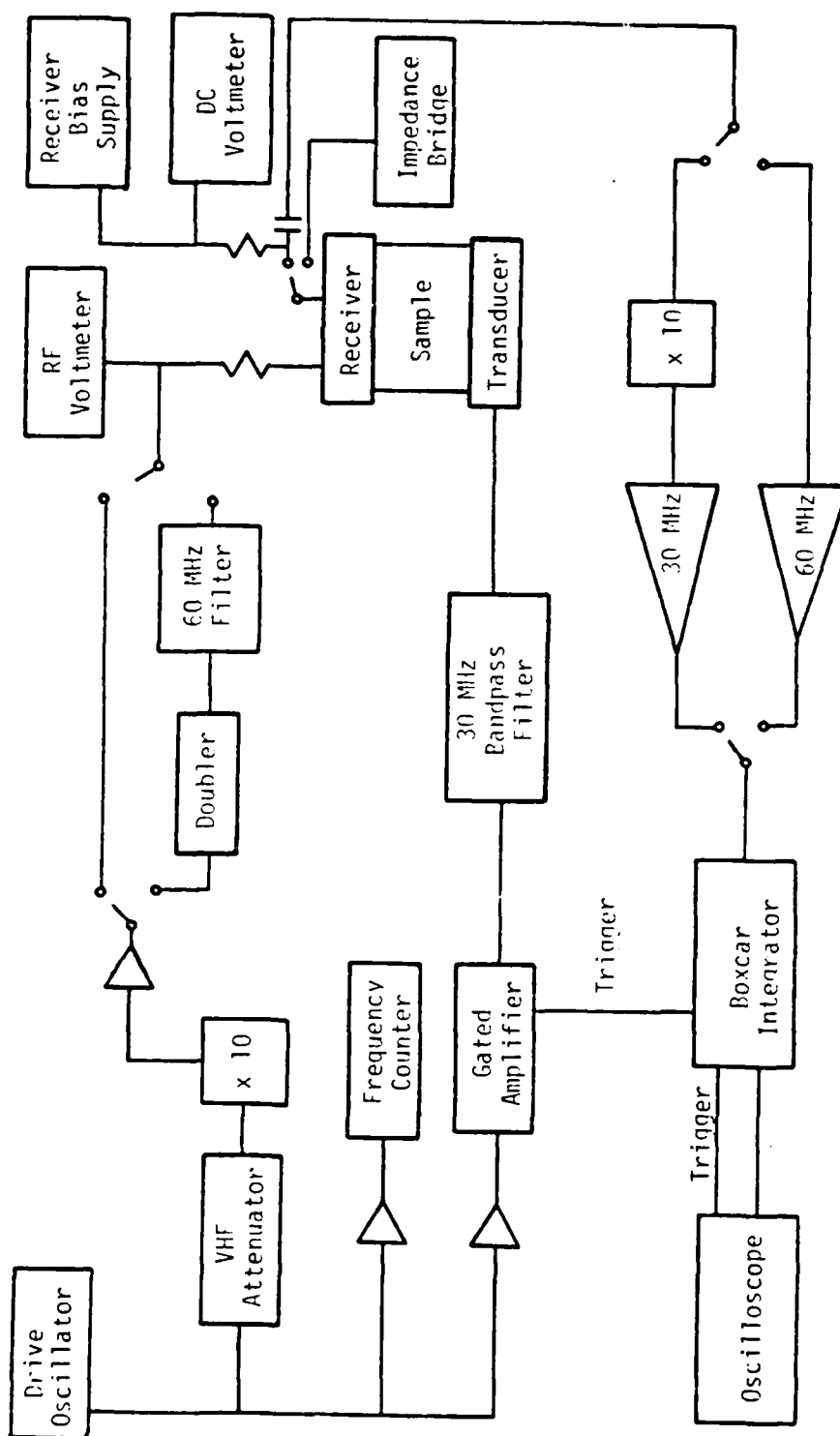
Figure III-5. Block diagram of the experimental arrangement used for the displacement amplitude measurements.
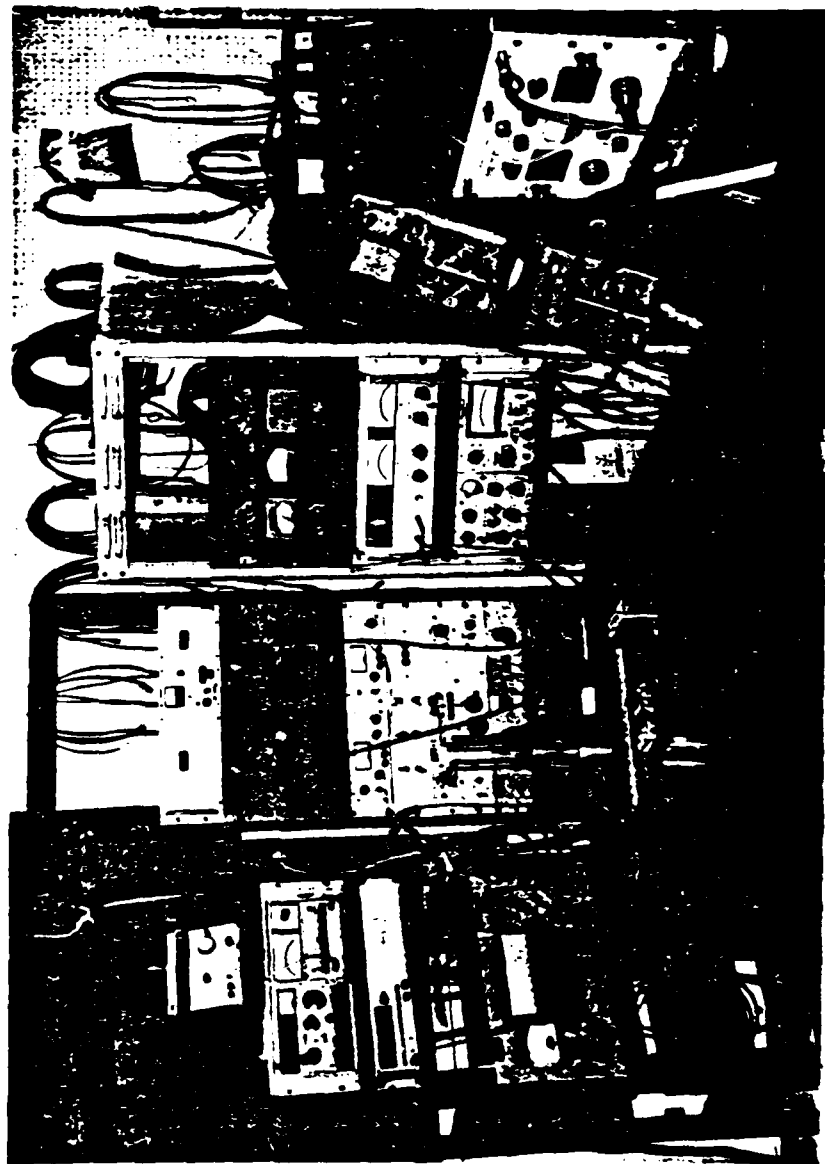
Figure III-6. Photograph of the experimental apparatus.

After removing the acoustic signal source a substitutional
signal is applied to give an output of the same magnitude as the
signal to be measured. The voltage across the signal generator is
measured with an RF voltmeter. For measurements of the second har-
monic, the fundamental frequency is doubled by a ring bridge mixer
and filtered with a 60 MHz bandpass filter.

The bias voltage applied to the detector is recorded and the gap
spacing of the receiver is measured by measuring its capacitance with
an impedance bridge. From the acquired data, the amplitude of the
fundamental and second harmonic are determined.

D. QUARTZ SAMPLES

The quartz samples were grown, oriented, and machined by the
Valpy-Fisher Corporation. A photograph of the samples is shown in
Figure III-7. A description of the quartz samples is given in
Table III-1. The axis of the crystals are oriented to within ($\pm.5°$).
The faces are lapped flat to within two fringes of light from a
helium discharge lamp and parallel to within 15 seconds of arc. The
cube was used to take measurements in the X-, Y-, and Z-directions.
It is adequate for measurements in the Z-direction and thus it will
be designated as the Z-cut sample. Measurements in the X-direction
indicated that a larger sample is required to enhance the low level
second harmonic. The cylindrical X-cut sample has a length of
1.5 inches. The receiving electrode as well as the quartz trans-
mitting transducer for the Z-cut quartz specimen is 0.765 cm in
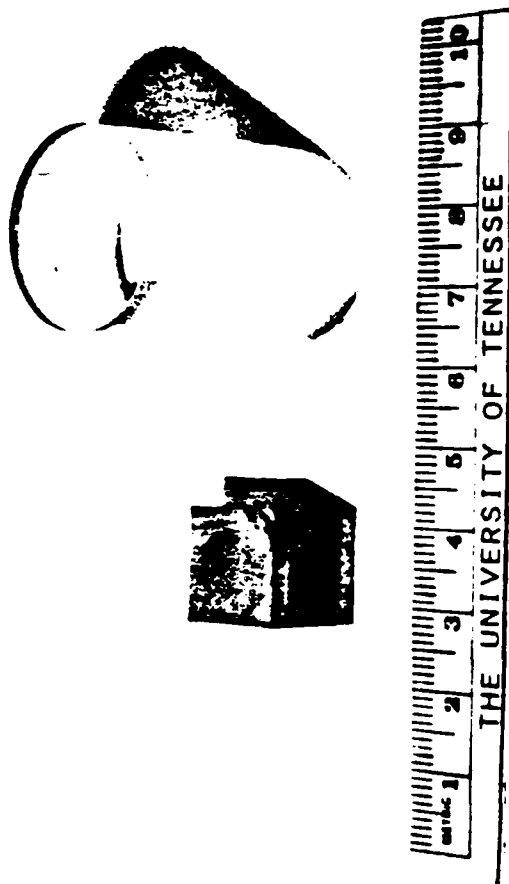
QUARTZ SAMPLES

Figure III-7. The quartz samples.

TABLE III-1

DESCRIPTION OF QUARTZ SAMPLES

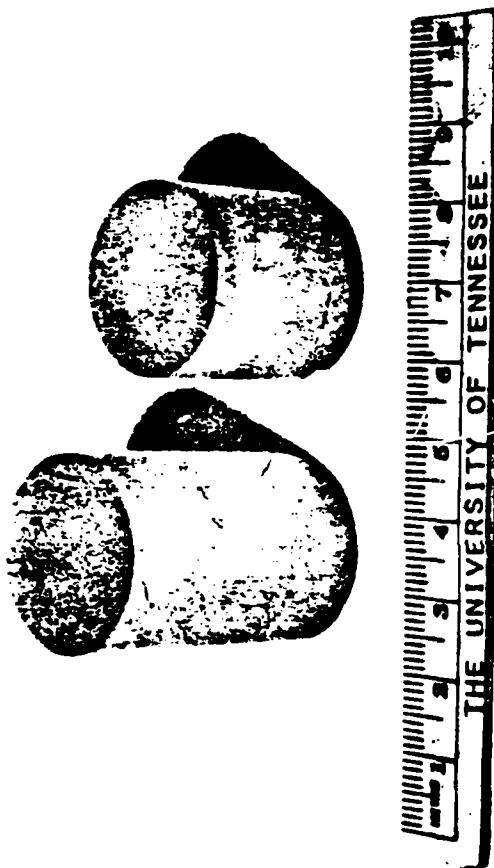| Principle Direction	Shape	Diameter (cm)	Length (cm)
Z	Cube		1.4938
X	Right circular cylinder		3.8386

diameter. In the case of the X-cut quartz specimen, they have a diameter of 1.269 cm.

E. LITHIUM NIOBATE SAMPLES

The lithium niobate samples were grown and oriented by Crystal Technology, Inc. They were acoustic grade $LiNbO_3$ which were machined into a right circular cylinder (Figure III-8). For the X-cut sample, the X-axis corresponded to the axis of the cylinder. Examination with crossed polaroids revealed no obvious strains. Similarly, for the Z-cut sample the Z-axis corresponds to the axis of the cylinder. The shapes and dimensions of the $LiNbO_3$ samples are listed in Table III-2. Observations of Philip and Breazeale (1982) indicated that it was desirable to obtain a longer Z-cut sample in order to enhance the extremely low level second harmonic observed along this direction. The Z-cut sample is 1.5" long. The specifications regarding orientation of crystalline axis flatness and parallelism are the same as for quartz. The diameter of the receiver electrode used for taking data with the lithium niobate samples is 1.269 cm.

F. PHASE MEASUREMENT

The phase of the second harmonic depends directly on the sign of the nonlinearity parameter β. A negative β indicates 180° phase difference from a positive β. A negative β is not to be expected in fluids, as this would violate the second law of thermodynamics (Lord Rayleigh, 1910). The situation is different in solids, however. An unambiguous proof of the existence of a negative β (in fused

LiNbO₃ SAMPLES

THE UNIVERSITY OF TENNESSEE.

Figure III-8. The LiNbO₃ samples.

TABLE III-2

DESCRIPTION OF LiNbO$_3$ SAMPLES

Principle Direction	Shape	Diameter (cm)	Length (cm)
X	Right circular cylinder	2.54	2.5561
Z	Right circular cylinder	2.54	3.8155

silica) exists (Bains and Breazeale, 1975). Although a negative β would be an unusual situation, it cannot be ruled out when one is investigating a new class of solid symmetry, as is the case here.

The general technique for determining the sign of β for an unknown sample is as follows:

1. A sample whose β is known to be positive is placed on the capacitive receiver.

2. The output of the capacitive receiver is examined with a phase sensitive detector.

3. Keeping everything constant, the known sample is replaced by an unknown.

4. A phase shift of 180° in the output of the phase sensitive detector indicates a negative β.

In these measurements a 100 MHz oscilloscope could actually be used as a phase sensitive detector since it had dual channel input with the possibility to add and subtract the two inputs. The experimental setup for the measurement is shown in Figure III-9. A Cu[111] sample having a known positive β is placed in the capacitive detector. The output from the capacitive receiver is fed into a directional coupler[*]

---

[*]The importance of using a directional coupler is that with a conventional power splitter one automatically loses 6 DB of signal in each of the two signal paths. A 6 DB loss for the low level second harmonic signal would reduce an already marginal signal-to-noise ratio. With the directional coupler, on the other hand, the loss is very small in one of the outputs and considerably greater in the other. The loss in the signal path carrying the 30 MHz fundamental signal can be great since that signal is extremely large compared with the second harmonic signal. Therefore, the directional coupler is a vital component in this experimental setup.
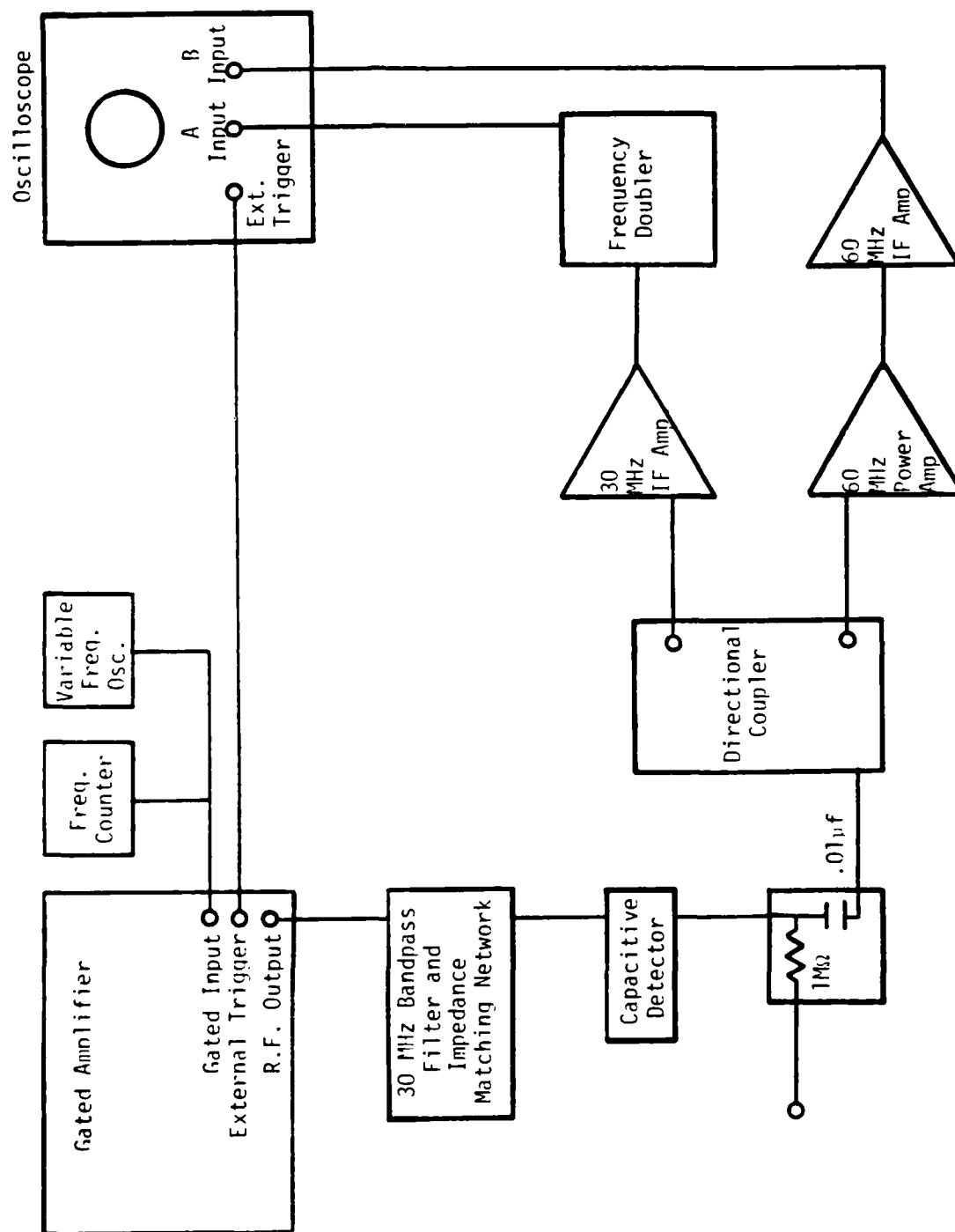
Figure III-9. Experimental apparatus for phase measurements.

which splits the signal into two parts. One of the signals from the directional coupler is fed into the 30 MHz IF amplifier. That signal is then frequency doubled and fed into channel A of the oscilloscope. The other signal from the directional coupler is fed into the 60 MHz power amplifier which is cascaded with the 60 MHz IF amplifier. The output of the 60 MHz IF amplifier then enters channel B of the oscilloscope. The display amplitude for channels A and B are adjusted to be approximately the same size. The time-coherent signals from channel A and B are then added together and the channel B invert control is activated. The result for the case of Cu[111] is that the added signal increases in size significantly. This indicates that one of the signals has undergone a phase shift of approximately 180° in passing through the amplifiers. For comparison, the Cu[111] sample is then removed and with everything kept constant the unknown is placed in the capacitive receiver. If the behavior is the same as copper, then the unknown β is positive. If the behavior is opposite to that of copper, then the unknown β is negative.

G. VELOCITY MEASUREMENTS

In order to determine K_2 one must either measure the velocity or use the appropriate combination of SOE constants from the literature. Reliable values of SOE constants exist for quartz, but not for $LiNbO_3$. Therefore, velocity measurements are necessary for $LiNbO_3$. The pulse overlap technique is used with the same experimental setup as shown in Figure III-5 (p. 42). The pulse width from the gated amplifier is broadened until an interference pattern is

produced. As the frequency of the VFO is changed, the pattern goes through a series of maxima and minima (Figure III-10). The minima are counted in a given frequency interval. The velocity c is then calculated from $c = \frac{2\Delta fL}{\Delta n}$ where Δf is the change in frequency corresponding to the number of minima Δn, and L is the length of the sample. The computed value for velocity is corrected for the presence of the transducer and bond by essentially the technique used by Williams and Lamb (1958).
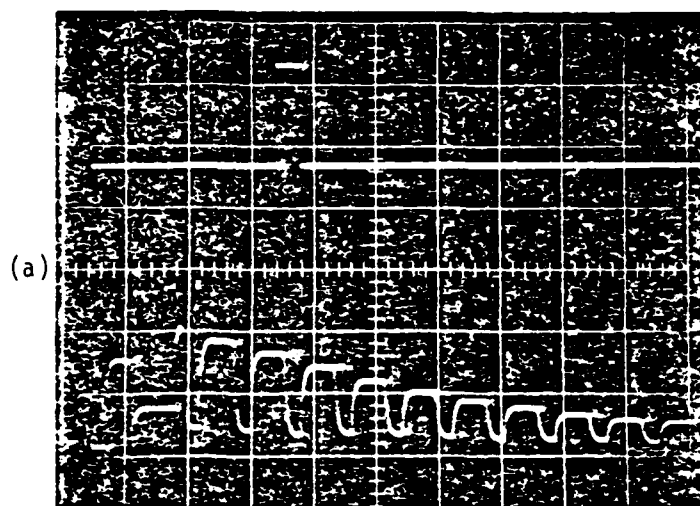
Minima in the interference pattern

Maxima in the interference pattern

Figure III-10. Echo overlap technique for velocity measurements.

CHAPTER IV

RESULTS AND DISCUSSION

In this chapter the results of measurement of the nonlinearity

parameters and TOE constants of quartz and $LiNbO_3$ are presented.

Most of the measurements were made with samples which are 1" diameter

right circular cylinders and transducers having a diameter of 1.27 cm.

In previous investigations with crystals of cubic symmetry this size

has been assumed to be large enough that the infinite plane wave

assumption is valid, so that no diffraction correction is necessary.

The present investigation shows that in fact diffraction causes a

perceptible change in the measured nonlinearity parameters of quartz

and $LiNbO_3$. Our data are corrected for diffraction. Interesting

and unexpected properties of quartz and $LiNbO_3$, such as a negative

nonlinearity parameter, are considered in connection with interpreta-

tion of the data.

A. NONLINEARITY MEASUREMENTS OF QUARTZ
IN THE Z-DIRECTION

The results of the measurements of nonlinear distortion of

ultrasonic waves in quartz in the Z-direction are listed in

Table IV-1. A plot of A_2 vs. A_1^2 is given in Figure IV-1. The line

drawn through the experimental points is the linear least squares fit

of data points. The correlation coefficient, given as a measure of

how well the line fits is defined as: correlation coefficient $= \dfrac{m\sigma_x}{\sigma_y}$

TABLE IV-1

AMPLITUDE OF ULTRASONIC WAVE COMPONENTS FOR Z-CUT QUARTZ AT ROOM TEMPERATURES

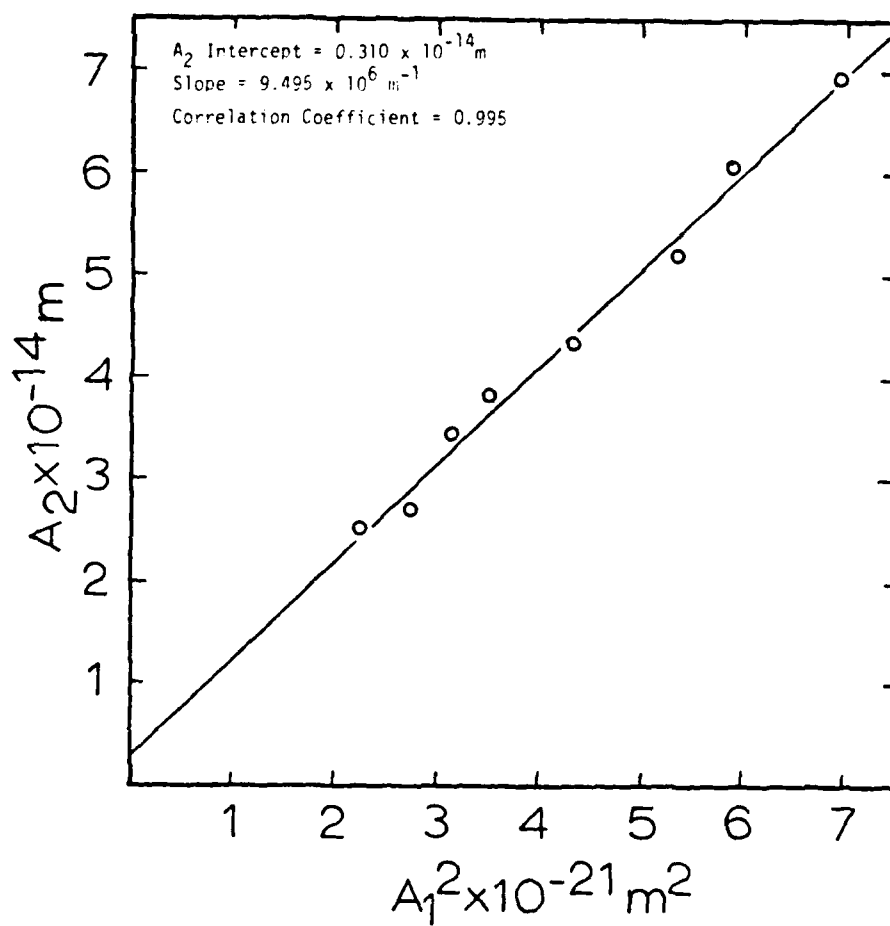| Sample Orientation	Frequency Used MHz	Fundamental Amplitude $\times 10^{-11}$ m	Second Harmonic Amplitude $\times 10^{-14}$ m	$\dfrac{A_2}{A_1^2}$ $\times 10^7$ m^{-1}	$\beta = 8 \dfrac{A_2}{A_1^2} \dfrac{1}{k^2 a}$ Uncorrected for Diffraction
Z	30.2955	4.738	2.514	1.120	6.066
		5.241	2.706	0.985	5.815
		5.588	3.455	1.106	6.529
		5.942	3.816	1.081	6.378
		6.615	4.350	0.994	5.865
		7.312	5.214	0.975	5.756
		7.677	6.068	1.174	6.929
		8.670	7.909	1.202	7.095

Figure IV-1. Graph of A_2 vs. A_1^2 for Z-cut quartz.

where m is the slope, σ_x is the standard deviation of the x array of data points, and σ_y is the standard deviation of the y array of data points. Possible values of the correlation coefficient may range from -1 to +1, with a perfect fit corresponding to either ±1. The value of .995 indicates an excellent fit. The fact that the line does not exactly intersect the origin results from residual amplifier noise (Bains, 1974) but does not have a perceptible effect on the evaluation of the nonlinearity parameter.

A plot of the nonlinearity parameter as a function of the fundamental amplitude is shown in Figure IV-2 in which an extrapolation to zero amplitude is made. The extrapolated curves approach the ordinate with a horizontal tangent (Yost, 1972). The extrapolated value of β_z is now corrected for diffraction. The diffraction correction which is used (Blackburn, 1981) is one in which the fundamental signal is corrected with linear theory. The effect of diffraction on the second harmonic is neglected as a first approximation. The correction is applied to the nonlinearity parameter of the Z-cut quartz sample in the following form:

$$\beta_{corrected} = \beta_{uncorrected} \; D_L^2$$

where D_L^2 = correction term. The value obtained from data in Table III-2 (p. 49), is used to evaluate this term. For the Z-direction in quartz D_L^2 = .8136. The uncorrected value of β_z = 6.00 was diffraction corrected to give a value of β_z = 4.88. This value is used with the SOE constants from the literature
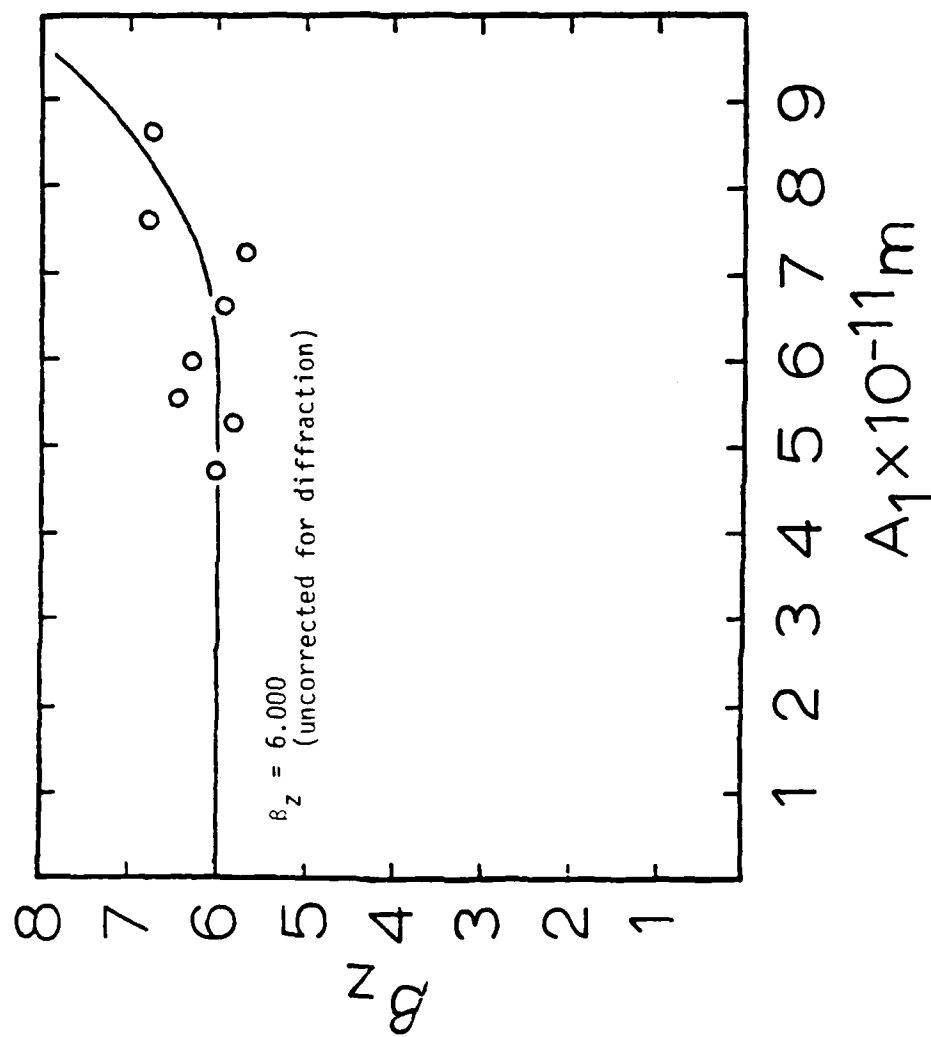
Figure IV-2. Graph of β_z vs. A_1 for Z-cut quartz.

$\beta_z = 6.000$
(uncorrected for diffraction)

(McSkimin et al., 1965) to calculate the TOE constant:

$$C_{333} = -8.34 \pm .55 \times 10^{12} \text{ dynes/cm}^2 .$$

B. NONLINEARITY MEASUREMENTS OF QUARTZ IN THE X-DIRECTION

The results of the measurements of the absolute amplitude of ultrasonic waves of quartz in the X-direction are listed in Table IV-2. A plot of A_2 vs. A_1^2 is given in Figure IV-3 in which the straight line is a least squares fit of the data. The correlation coefficient of 0.9995 indicates an almost perfect fit of the data and the intercept is even smaller than observed in Figure IV-1 (p. 57). The size of the samples and transducer used for all other measurements were great enough that the plane wave approximation would have contributed a certain amount of systematic error. In order to eliminate this approximation, the diffraction correction was applied in each case. The uncorrected nonlinearity parameter β_x was plotted versus A_1 in Figure IV-4. The curve is extrapolated to zero amplitude to give the most reliable value for the uncorrected $\beta_x = -.636$. The correction factor is $D_L^2 = .8263$. Therefore, the diffraction corrected value is $\beta_x = -.526$. The experimental value of β and the SOE constants from the literature (McSkimin et al., 1965) are used to calculate $C_{111} = 2.15 \pm .06 \times 10^{12} \text{ dynes/cm}^2$. The C_{111} constant for quartz is, strictly speaking, the piezoelectrically stiffened coefficient. However, Thurston et al. (1966) found the piezoelectric contribution to quartz in the X-direction to be within their experimental error.

61

TABLE IV-2

AMPLITUDE OF ULTRASONIC WAVE COMPONENTS FOR X-CUT QUARTZ AT ROOM TEMPERATURES

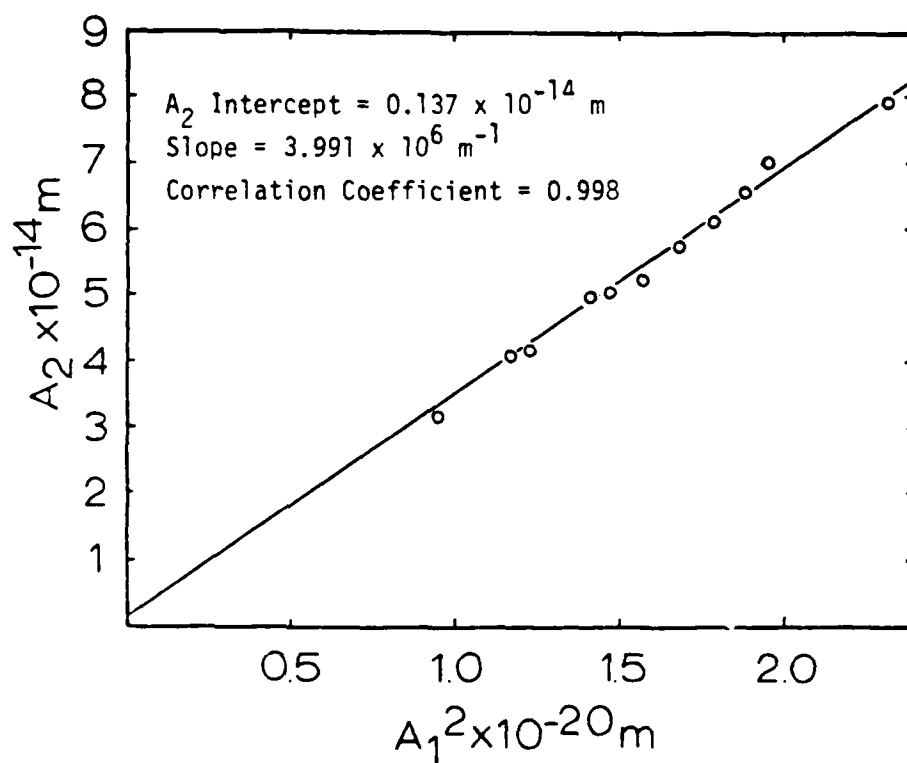| Sample Orientation	Frequency Used	Fundamental Amplitude $\times 10^{-10}$ m	Second Harmonic Amplitude $\times 10^{-14}$ m	$\dfrac{A_2}{A_1^2}$ $\times 10^6$ m^{-1}	$\beta = 8\dfrac{A_2}{A_1^2}\dfrac{1}{k^2 a}$ Uncorrected for Diffraction
X	30.2975	0.973	3.334	3.518	-0.656
		1.086	4.109	3.483	-0.549
		1.108	4.343	3.539	-0.671
		1.119	4.901	3.476	-0.615
		1.205	5.095	3.509	-0.665
		1.255	5.429	3.444	-0.653
		1.297	5.776	3.435	-0.640
		1.339	6.222	3.473	-0.658
		1.378	6.563	3.458	-0.612
		1.401	7.001	3.565	-0.631
		1.525	7.930	3.380	-0.597
		1.654	9.845	3.598	-0.636

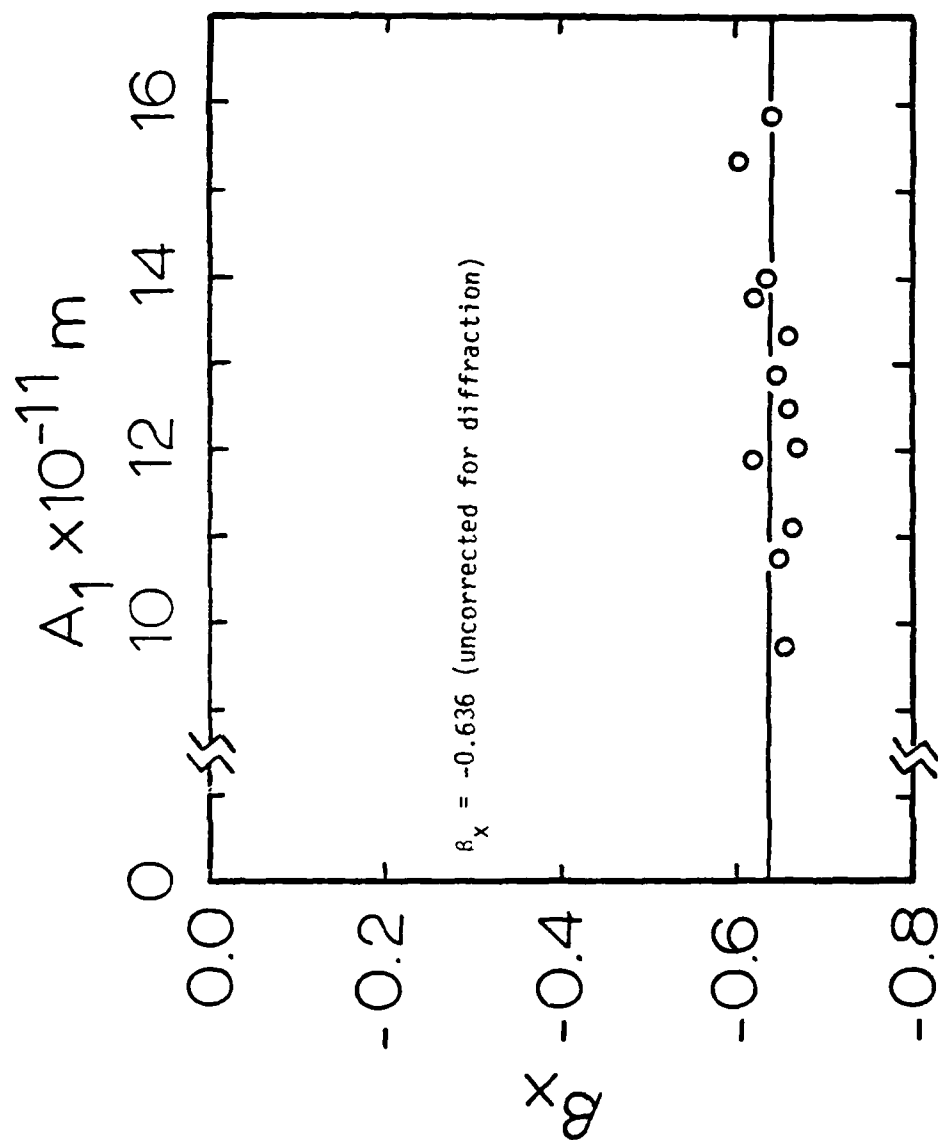Figure IV-3. Graph of A_2 vs. A_1^2 for X-cut quartz.

63

Figure IV-4. Graph of β_x vs. A_1 for X-cut quartz .

Similarly, no distinction is made here between the constant field coefficient of X-cut quartz and the effective coefficient.
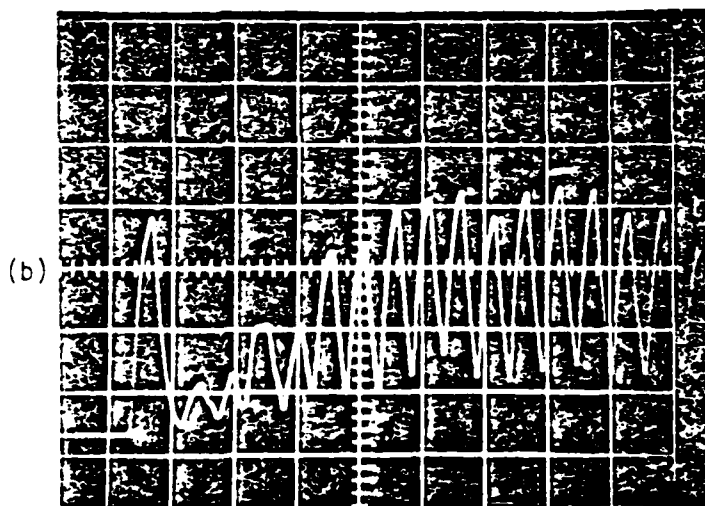
C. THE BEHAVIOR OF QUARTZ IN THE Y-DIRECTION

The Y-direction for crystals having trigonal symmetry is not a longitudinal pure mode direction. The Y-direction corresponds to a quasilongitudinal mode coupled to a shear mode. As a consequence of this coupling, no quantitative data for the determination of TOE constants can as yet be obtained in this direction using the capacitive detector. However, the Y-direction for both quartz and lithium niobate made a very distinctive and easily recognized pattern using the capacitive detector. A comparison of the behavior in the Z-direction with that in the Y-direction is given in Figure IV-5.

In the Z-direction in which a longitudinal wave propagates, the amplitude decays exponentially. In contrast, in the Y-direction in quartz the amplitude increases to a maximum value, then decreases. Evidentally there is very little energy initially in the longitudinal mode but upon successive reflections the pulse amplitude grows, apparently as a result of mode conversion upon reflection. The amplitude decreases, probably as a result of both attenuation and the conversion of energy back into the transverse mode (which is not detected by the capacitive receiver).
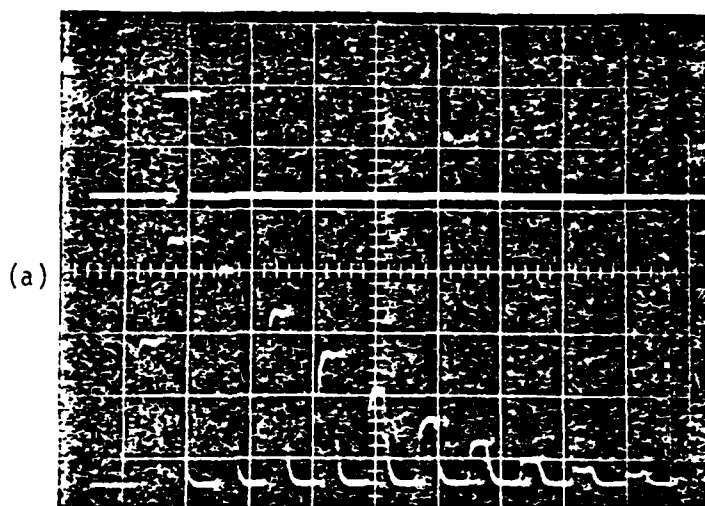
Typical pulse train for a pure
mode longitudinal wave

Typical pulse train for coupled modes
in the Y-direction of quartz

Figure IV-5. A comparison of the pulse train for quartz in the
Z- and Y-directions.

D. DISCUSSION OF RESULTS FOR QUARTZ

Measured values of the nonlinearity parameter of quartz are listed in Table IV-3, where β_X for quartz in the X-direction is found to be negative, an unusual situation. The fact that β is negative in this case was concluded from evaluation of the data of Thurston et al. (1966) and comparing with our measured data. Such a behavior has been observed only once before, with fused silica (Bains and Breazeale, 1975). It has not been observed with crystals having cubic symmetry and hence is of considerable importance to the interpretation of data on trigonal crystals. This behavior implies that the second harmonic is 180° out of phase with the fundamental and hence the distortion of the wave form is toward a backward sawtooth wave instead of the usual forward sawtooth encountered in the case of a positive nonlinearity parameter. The phase of the second harmonic is not routinely determined in the experiments. For fused silica this behavior implies that C_{111} is positive; however, in quartz C_{111} still is negative, as can be seen from the expression $C_{111} = -C_{11}(3 + \beta)$.

If $|\beta| < 3$, then a negative β will not cause a reversal in the sign of C_{111}. However, if $|\beta| > 3$, then, a negative ε implies a positive C_{111}. In the measurements, then, a misinterpretation of the sign of β can cause errors in both the sign and the magnitude of C_{111} for crystals of trigonal symmetry! Our measured velocities in the quartz samples agree very closely with those given by McSkimin et al. (1965). McSkimin's SOE constants therefore were used for the calculation of the TOE constants in this experiment. The SOE constants,

TABLE IV-3

VALUES OF THE NONLINEARITY PARAMETERS FOR QUARTZ

Sample Orientation	β
Z	4.88
X	-0.526

along with the calculated TOE constants of quartz are listed in Table IV-4. The uncertainties listed with the constants are the random uncertainties. They were calculated from the standard deviation in the nonlinearity parameter. The random error was somewhat greater for the Z-direction than the X-direction because the small cube-shaped samples were harder to align than the large cylindrical samples. Measurement of the TOE constants of quartz made by Thurston et al. (1966) using the hydrostatic pressure technique are also presented in Table IV-4, as are those of Stern and Smith (1968) who used a modification of the uniaxial stress-hydrostatic pressure technique.

The agreement among the three sets of data indicates that the harmonic generation technique is capable of producing dependable values of C_{111} and C_{333} for crystals of trigonal symmetry. The disagreement ranges from less than 1% to approximately 2.5%. The random error of these measurements is less than 6.5% as indicated.

These data represent the first set of measurements of both C_{111} and C_{333} for crystals having trigonal symmetry using the capacitive detector. The close agreement with the measurements made of two

TABLE IV-4

SECOND-ORDER ELASTIC CONSTANTS AND THIRD-ORDER ELASTIC CONSTANTS FOR QUARTZ ALONG
THE PRINCIPAL DIRECTIONS AT ROOM TEMPERATURE

Sample Orientation	SOE Constants $\times 10^{11}$ dynes/cm^2 McSkimin et al. (1965)	TOE Constants $\times 10^{12}$ dynes/cm^2		
		Present Experiment	Thurston et al. (1966)	Stern and Smith (1968)
X	$C_{11} = 8.680$	$C_{111} = -2.15 \pm .06$	$C_{111} = -2.10 \pm .07$	$C_{111} = -2.18$
Z	$C_{33} = 10.575$	$C_{333} = -8.34 \pm .55$	$C_{333} = -8.15 \pm .18$	$C_{333} = -8.37$

independent groups using different techniques also verifies the
validity of the perturbation solution of the nonlinear equation for
trigonal symmetry obtained by Philip (1983).

E. THE SOE CONSTANTS OF LiNbO$_3$

The value K$_2$ may be calculated from the measured velocity
and density of a sample or, alternatively, one may use a reliable SOE
constant from the published literature. If there is good quality
control of the material; i.e., no sample dependence, then there
should be almost no variation in the observed SOE constants from
sample to sample or from independent measurements. However, there
was a noticeable variation in the SOE constants of LiNbO$_3$ reported
in the literature as illustrated in Table IV-5. Therefore as a
result of this variation the K$_2$ were determined by direct measurement
of ultrasonic wave velocities in the samples used for measurement of
nonlinearity parameters. The results are listed in Table IV-5. The
SOE constants calculated in this experiment are somewhat lower than
the SOE constants given by Philip and Breazeale (1982) and Nakagawa
et al. (1973). In both of these cases, the density of lithium
niobate was quoted as being $\rho = 4.7$ gm/cm^3 instead of the more
accurate value of $c = 4.644$ gm/cm^3 (Cook and Jaffe, 1979).
If a density of $c = 4.644$ is used to calculate the SOE constants of
Philip and Breazeale (1982) and Nakagawa et al. (1973), then there is
a close agreement with the SOE constants used in the present work as
illustrated in Table IV-6.

TABLE IV-5

VELOCITIES AND SOE CONSTANTS OF LiNbO$_3$*

	Velocity Z-Direction x 10^5 cm/sec	Velocity X-Direction x 10^5 cm/sec	c_{11}^E x 10^{12} dynes/cm^2	c_{33}^D x 10^{12} dynes/cm^2	c_{33}^E x 10^{12} dynes/cm^2
Present experiment**	7.306 ± .012	6.536 ± .020	1.98 ± .01	2.48 ± .008	-
Nakagawa et al. (1973)			2.0	2.51	2.43
Philip and Breazeale (1982)		6.5032	1.988		
Smith and Welsh (1971)			2.030	2.495	2.424
Warner et al. (1967)			2.03	2.52	2.45

*The superscript D indicates the effective or stiffened values. The superscript E indicates the constant field value.

**Density ρ = 4.644 (Cook and Jaffe, 1979).

TABLE IV-6

SOE CONSTANTS OF $LiNbO_3$ USING DENSITY ρ = 4.644 gm/cm^3

	c_{11}^E x 10^{12} dynes/cm^2	c_{33}^D x 10^{12} dynes/cm^2
Present experiment	1.98	2.48
Nakagawa et al. (1973)	1.98	2.48
Philip and Breazeale (1982)	1.964	

F. NONLINEARITY MEASUREMENTS OF LITHIUM
NIOBATE IN THE X-DIRECTION

The results of the measurement of nonlinear distortion of waves
in lithium niobate in the X-direction are listed in Table IV-7. The
plot of A_2 vs. A_1^2 for this sample is given in Figure IV-6. The line
through the data points is a least squares fit of the data. The
correlation coefficient of .9996 indicates an almost perfect fit of
the data. The intercept indicates that residual noise is very small.
The plot of the nonlinearity parameter β_x vs. A_1, the fundamental
amplitude, appears in Figure IV-7. The curve is extrapolated to zero
amplitude to give the most reliable value for β_x. The uncorrected
value for β_x is $\beta_x = 7.11$. With a diffraction correction factor
$D_L^2 = .8446$, the corrected value for β_x is $\beta_x = 6.01$. The relative
value of the TOE constant is calculated to be $C_{111} = -17.83 \pm$
$.35 \times 10^{12}$ dynes/cm^2.

During the process of taking data, a very strong second harmonic
was observed with X-cut lithium niobate. The magnitude of the second
harmonic was much larger than one would expect based on the value of
C_{111} reported by Nakagawa et al. (1973). Therefore, a photograph was
taken (Figure IV-8) to illustrate the strong second harmonic found
with our samples. Both the fundamental and second harmonic are
illustrated. The second harmonic is approximately three times as
large as would be expected from Nakagawa's value of C_{111}. The slow
decrease in amplitude in the fundamental pulse train results from
the very low attenuation in LiNbO$_3$. This peculiar property in the

TABLE IV-7

AMPLITUDE OF ULTRASONIC WAVE COMPONENTS FOR X-CUT LITHIUM NIOBATE AT ROOM TEMPERATURES

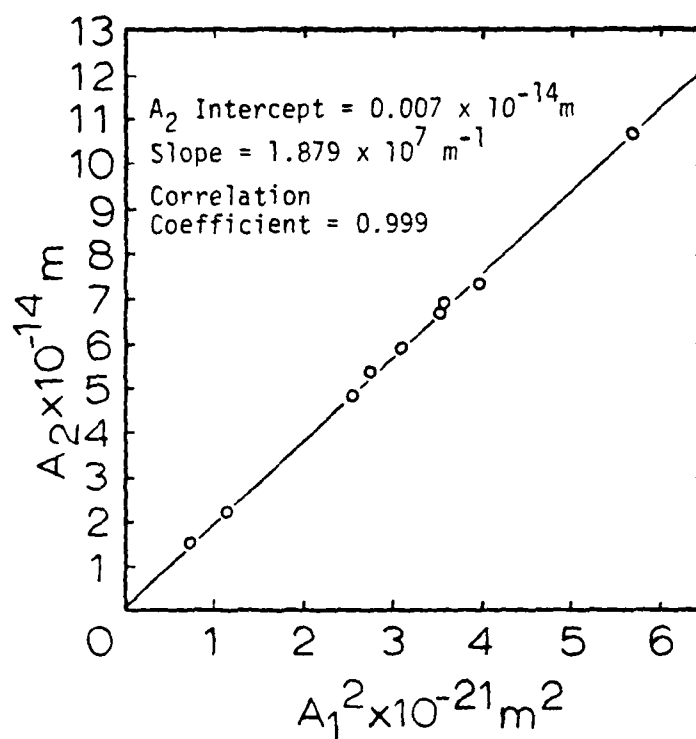| Sample Orientation	Frequency Used MHz	Fundamental Amplitude $\times 10^{-11}$ m	Second Harmonic Amplitude $\times 10^{-14}$ m	$\dfrac{A_2}{A_1^2}$ $\times 10^7$ m^{-1}	$\beta = 8 \dfrac{A_2}{A_1^2} \dfrac{1}{k^2 a}$ Uncorrected for Diffraction
X	30.0802	2.826	1.577	1.975	7.374
	30.0802	3.422	2.254	1.925	7.188
	30.2280	5.085	4.916	1.901	7.020
	30.2280	5.272	5.463	1.965	7.283
	30.2280	5.591	5.989	1.916	7.102
	30.2280	5.936	6.734	1.011	7.083
	30.2280	5.943	6.872	1.946	7.213
	30.2280	6.312	7.392	1.855	6.875
	30.2280	7.550	10.792	1.893	7.017

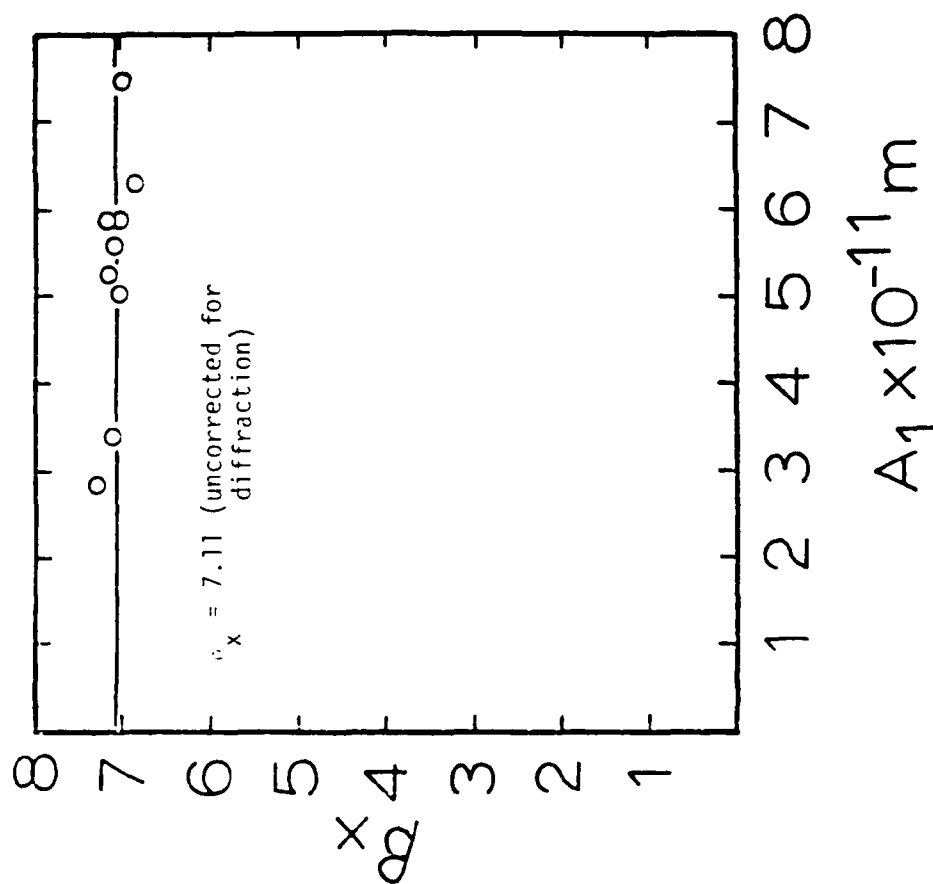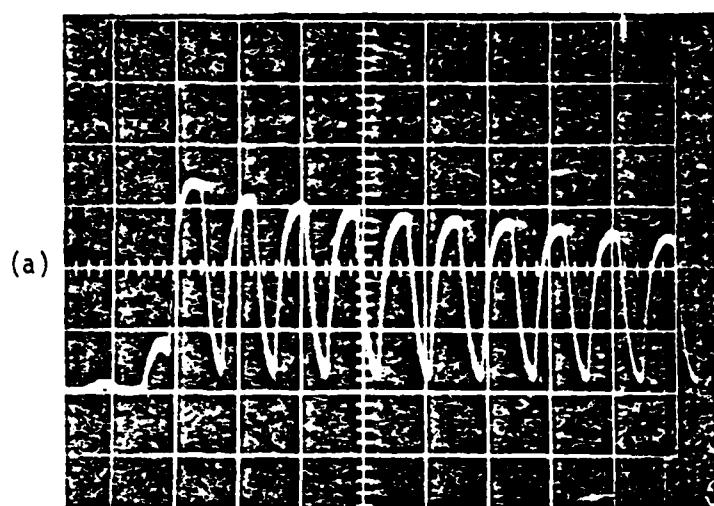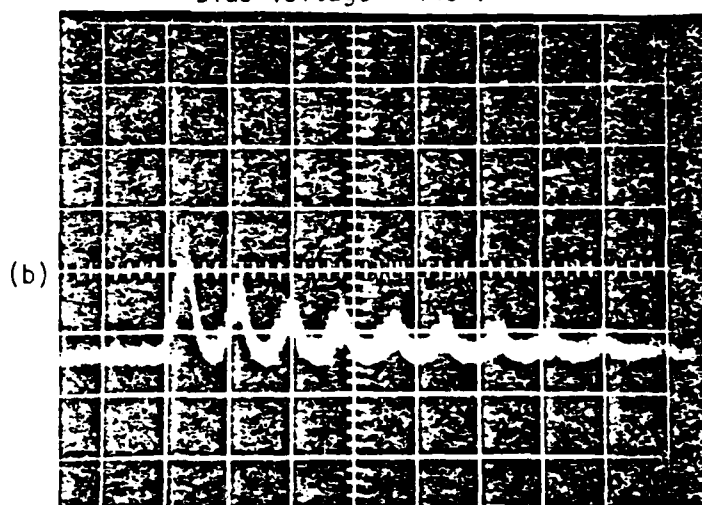Figure IV-6. Graph of A_2 vs. A_1^2 for X-cut $LiNbO_3$.

Figure IV-7. Graph of β_x vs. A_1 for X-cut LiNbO$_3$.

Fundamental, 1 V/cm, 10µsec/cm;
Bias voltage = 140 V

Second harmonic, .02 V/cm, 10µsec/cm;
Bias voltage = 140 V

Figure IV-8.   The fundamental and second harmonic signal from
X-cut lithium niobate.

material is confirmed by the data of Spencer et al. (1965). The two

pulse trains in Figure IV-8 illustrate the point that the growth of

a large second harmonic is not necessarily associated with a large

attenuation coefficient for the fundamental.

G. VALUES OF NONLINEARITY PARAMETER AND TOE CONSTANTS OF $LiNbO_3$ IN THE Z-DIRECTION

The results of the measurement of absolute amplitude of the

fundamental and second harmonic of ultrasonic waves in lithium

niobate in the Z-direction are presented in Table IV-8. The relation-

ship of A_2 to $A_1{}^2$ is plotted in Figure IV-9. The correlation

coefficient indicates an excellent linear fit. The increase in the

scatter of the data results from the extremely small second harmonic

signal observed in the Z-direction. The small intercept indicates the

very small residual noise. The relationship β_x vs. A_1 is plotted in

Figure IV-10 and the curve is extrapolated to zero amplitude to yield

the most reliable uncorrected value for β_z which is $\beta_z = 0.444$. The

diffraction factor is $D_L{}^2 = .8082$; therefore, the corrected value

for β_z is $\beta_z = .359$. The assignment of the sign of β_z and hence the

evaluation of $C_{333} = -8.42 \pm .16 \times 10^{12}$ dynes/cm^2 results from a phase

measurement described in the next section.

H. EVALUATION OF THE SIGN OF β_z FOR $LiNbO_3$

In contrast to the situation in quartz, the data of Nakagawa

did not allow an unambiguous assignment of the sign of β_z for $LiNbO_3$.

TABLE IV-8

AMPLITUDE OF ULTRASONIC WAVE COMPONENTS FOR Z-CUT LITHIUM NIOBATE AT ROOM TEMPERATURES

Sample Orientation	Frequency Used MHz	Fundamental Amplitude $\times 10^{-10}$ m	Second Harmonic Amplitude $\times 10^{-14}$ m	$\frac{A_2}{A_1^2}$ $\times 10^6$ m^{-1}	$\beta = 8 \frac{A_2}{A_1^2} \frac{1}{k^2 a}$ Uncorrected for Diffraction
Z	30.1062	1.029	1.487	1.406	0.438
	30.0850	1.051	1.609	1.455	0.454
	30.1062	1.099	1.652	1.368	0.426
	30.1062	1.138	1.861	1.434	0.447
	30.1062	1.211	2.133	1.450	0.452
	30.1107	1.226	2.145	1.428	0.445
	30.1107	1.261	2.227	1.399	0.436
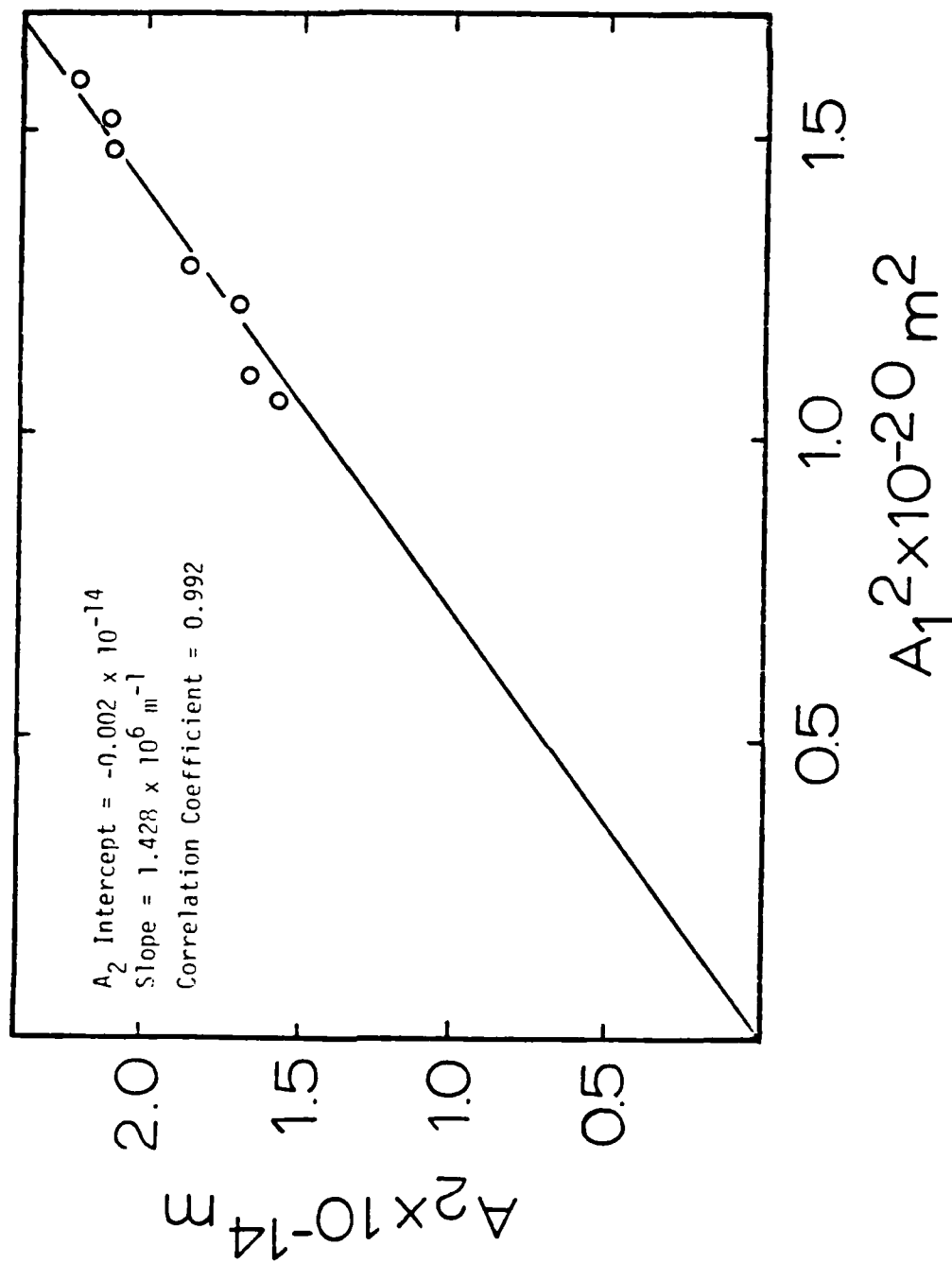
Figure IV-9. Graph of A_2 vs. A_1^2 for Z-cut $LiNbO_3$.

A_2 Intercept = -0.002 x 10^{-14}
Slope = 1.428 x 10^6 m^{-1}
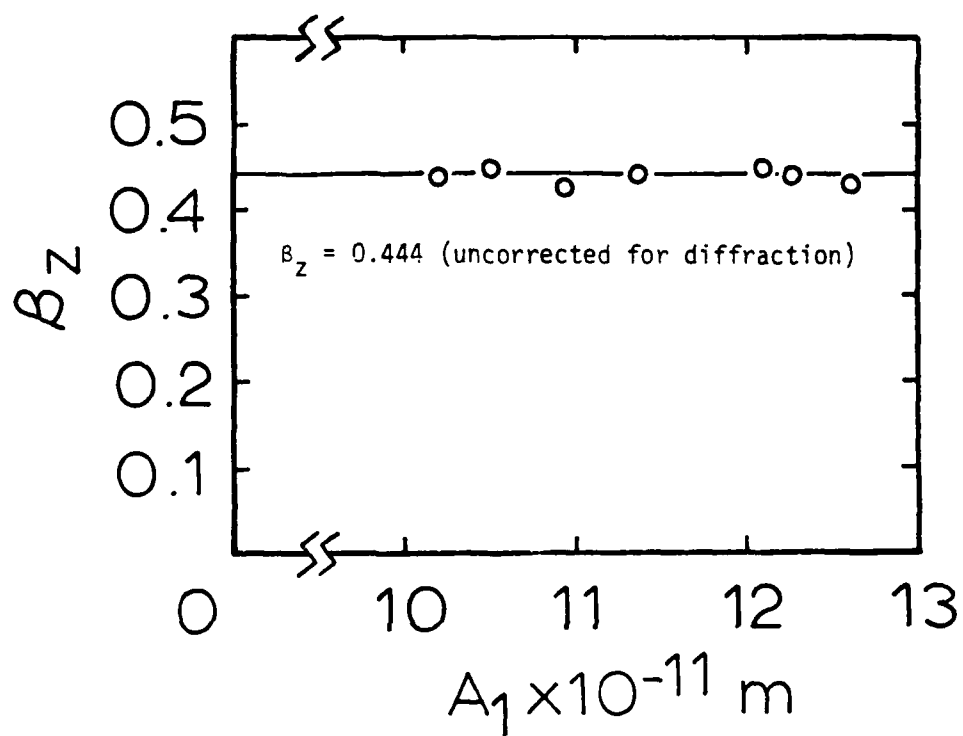Correlation Coefficient = 0.992

Figure IV-10. Graph of β_z vs. A_1 for Z-cut LiNbO$_3$.

Therefore, it is necessary to determine the sign of β_z by direct measurement. Results of the measurement of the phase of Z-cut lithium niobate by the comparison procedure (Chapter III) are illustrated in Figure IV-11. It is noted that the behavior for Z-cut lithium niobate is exactly analogous to the behavior of Cu[111]. The effect is not as pronounced for Z-cut lithium niobate as that for Cu[111] as a result of the comparatively smaller second harmonic. The fact that β for Cu[111] is known to be positive indicates that the β for Z-cut lithium niobate is also positive. This particular measurement is difficult as a result of the very small second harmonic signal observed in the Z-direction of $LiNbO_3$.

I. DISCUSSION OF RESULTS FOR $LiNbO_3$

The measured values of the nonlinearity parameters for lithium niobate are listed in Table IV-9. The definition of the nonlinearity parameter presented in this work is consistent with the corresponding definition for liquids and gases. [It is a factor of three greater than the expression used by Philip and Breazeale (1982).] The calculated TOE constants for both X- and Z-directions in lithium niobate are listed in Table IV-10.

First consider the X-direction. The standard deviation in C_{111} is of the order of 2%. Since the same procedure and setup was used for $LiNbO_3$ as for quartz, the systematic error should be of the same order of magnitude. Therefore, the probable systematic errors should be no greater than approximately 3%. Only two known published values
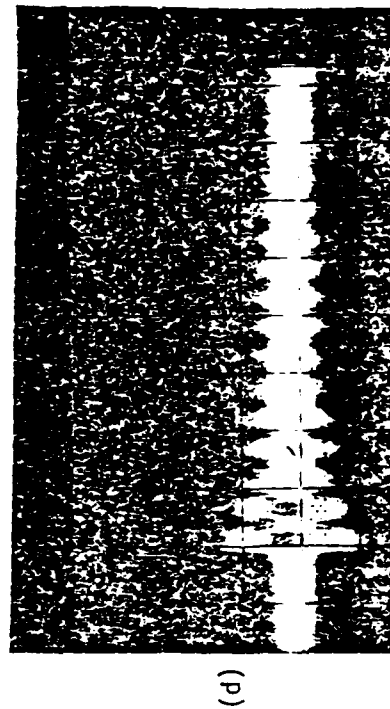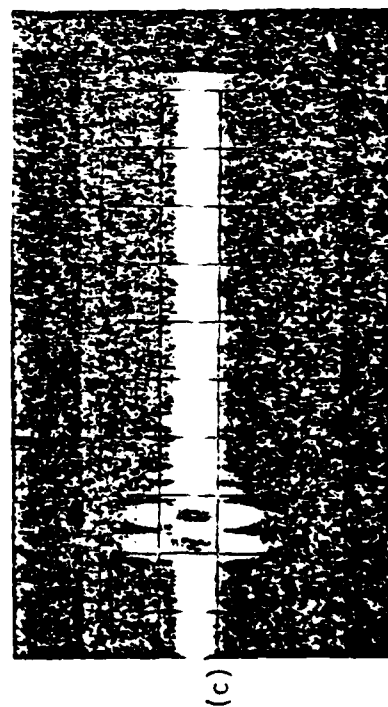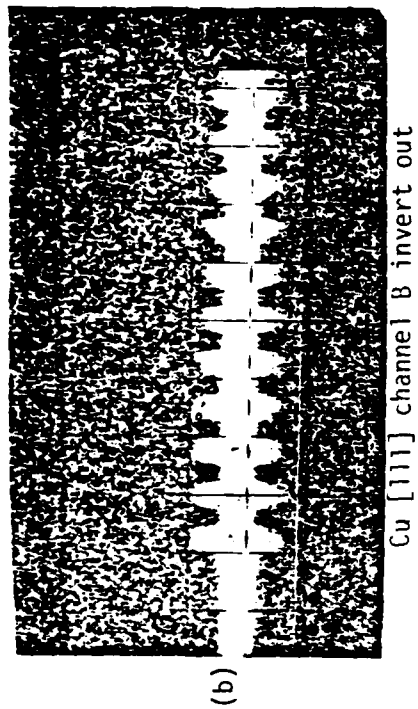
(b) Cu [111] channel B invert out

(d) Z-cut LiNbO$_3$ channel B invert out

(a) Cu [111] channel B invert activated

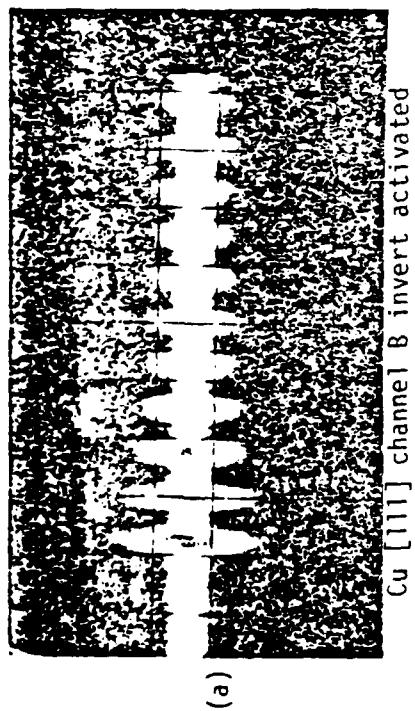(c) Z-Cut LiNbO$_3$ channel B invert activated

Figure IV-11. The phase measurement of Z-cut LiNbO$_3$.

TABLE IV-9

VALUES OF THE NONLINEARITY PARAMETER ε FOR LITHIUM
NIOBATE (CORRECTED FOR DIFFRACTION)

Sample Orientation	ε
X	6.01
Z	0.359

TABLE IV-10

THIRD-ORDER ELASTIC CONSTANTS OF LiNbO$_3$

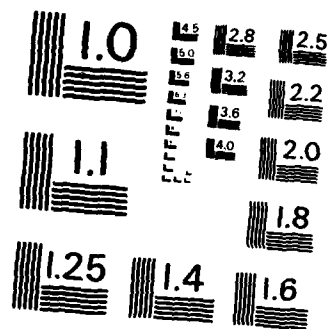|	C_{111}^E $\times 10^{12}$ dynes/cm^2	C_{333}^D $\times 10^{12}$ dynes/cm^2	C_{333}^E $\times 10^{12}$ dynes/cm^2
Present experiment	-17.83 ± .35	-8.33 ± .15	-3.63 ± 6.90*
Nakagawa et al. (1973)	-5.12 ± 1.94		
Philip and Breazeale (1982)	-16.1		

*This value includes one term in addition to the constant field coefficient.

MICROCOPY RESOLUTION TEST CHART
NATIONAL BUREAU OF STANDARDS-1963-A

(Nakagawa et al., 1973; Philip and Breazeale, 1982) are available for comparison with the present measurement of C_{111}.

The measurement completed in this experiment indicates a value for C_{111} approximately three times larger than the value given by Nakagawa et al. (1973). Considering the large magnitude of the SOE constants in the X-direction, a value for C_{111} of the order of magnitude suggested by Nakagawa et al. would imply a very low level second harmonic signal. However, that is contrary to the very strong second harmonic signal illustrated in Figure IV-8 (p. 76).

The values of C_{111} given by Philip and Breazeale (1982) are 10% lower than measured in this investigation. This difference in part may result from actual differences in the samples themselves. There are indications of some sample dependence in the value of the SOE constants and hence there may be sample-dependent variations in the TOE constants as well. Refinements in crystal growing techniques took place in the late 1970s (Räuber, 1978). The sample measured by Philip and Breazeale (1982) was grown in 1975 by Union Carbide. Our samples were grown in 1982 by Crystal Technology. Since $LiNbO_3$ crystals are susceptible to a number of defects such as grains canted by 1 or 2 degrees and/or dislocations, efforts recently have been directed toward reduction of defect density during crystal growth. The very best crystals are thought still to have surface dislocation densities from 10^3 to $10^4/cm^2$ (Räuber, 1978). Variation in dislocation density can make the harmonic generation measurement of the TOE constants material dependent (Truell et al., 1969; Hikata et al., 1965). It is possible,

therefore, that the harmonic generation technique we have used could serve as a sensitive nondestructive test for quality control in the manufacture of $LiNbO_3$ crystals. In order to make this test feasible one would need to correlate magnitude of β with dislocation density.

Consider next the measurements made on Z-cut $LiNbO_3$. Since the Z-direction in $LiNbO_3$ is a piezoelectrically active direction, the TOE constant given in·the present work is the piezoelectrically stiffened coefficient. The standard deviation of the data is 2%; the systematic error is estimated to be 3%. Therefore the total error is of the order of 5%. No comparison is made with Nakagawa's value for this TOE constant for a number of reasons. First, Nakagawa's large error bars (two times the value of the quantity measured) for this coefficient make a comparison impractical. Second, Nakagawa subtracts some of the coupled terms in an attempt to approximate a constant field coefficient; however, one of those terms (whose magnitude is unknown) is left imbedded in the expression for the constant field coefficient.

One peculiar characteristic of Z-cut $LiNbO_3$ is the very low level second harmonic generated. The small value given for β_z (Table IV-9, p. 83) indicates that lithium niobate in the Z-direction more closely approximates a linear solid than any other material that has been previously studied.

Of equal interest is the fact that the second harmonic for X-cut quartz was also very low. Both of these examples indicate that a very small second harmonic is present in the direction of piezoelectric

stiffening. This should be checked with other piezoelectric trigonal crystals to determine whether or not this is a general property.

Philip and Breazeale (1982) first observed with a capacitive receiver the fact that a strong piezoelectrically coupled solid, i.e., lithium niobate, produced a signal with no bias voltage applied to the detector. This effect was observed in the Z-direction and also in the Y-direction (in which coupled modes appear that are strongly piezoelectrically stiffened). A similar effect was observed with the Z-cut $LiNbO_3$ sample used in this work. A comparison of the fundamental signal from Z-cut lithium niobate with and without bias voltage applied is illustrated in Figure IV-12. It is conceivable that the signal without bias could represent the piezoelectric contribution to the third-order elastic behavior. The effective TOE constant takes the following form:

$$c_{333}^D = c_{333}^E + \text{(piezoelectrically coupled terms)} .$$

If the piezoelectric contribution could be subtracted from the effective TOE constant reported in this work, the constant field coefficient could be evaluated. The measured ratio of the piezoelectric contribution to the total fundamental amplitude is .35. The contribution to the second harmonic without bias is too small to be measured with existing instrumentation.

Philip actually observed the strongly piezoelectrically stiffened second harmonic signal in the Y-direction both with and

(a)
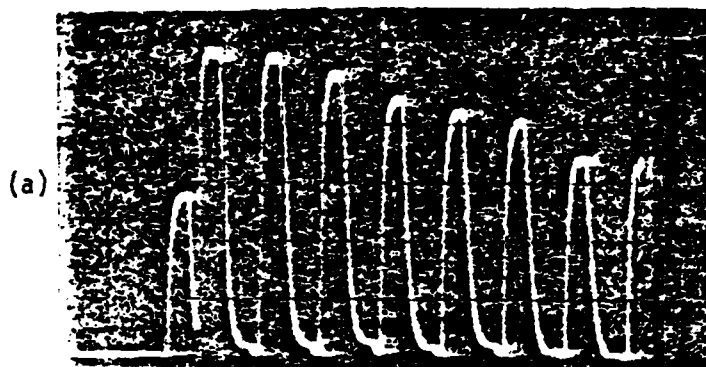
Fundamental with bias voltage 1 V/cm

(b)

Fundamental without bias voltage .5 V/cm

Figure IV-12. A comparison of the fundamental ultrasonic signal from $LiNbO_3$ with bias voltage applied and without bias voltage applied.

without bias applied to the capacitive detector. It is to be assumed that an adequate refinement of the apparatus would allow one to observe the piezoelectrically stiffened second harmonic in the other piezoelectrically active directions in which it is so small.

J. SUMMARY AND CONCLUSIONS

The nonlinearity parameters and TOE constants of quartz and lithium niobate have been measured and compared with similar measurements published in the literature. Measurements in quartz have produced results which agree closely with values published prior to this work (Thurston et al., 1966; Stern and Smith, 1968). This should serve to verify the validity of the perturbation solution of the nonlinear equation in the X- and Z-directions for trigonal symmetry and to demonstrate that the use of the capacitive detector provides reliable data for crystals of trigonal symmetry.

Measurements in $LiNbO_3$ have yielded results which disagree with the measurements reported by Nakagawa et al. (1973). A comparison of the present results with Philip and Breazeale (1982) and the variation of SOE constants indicates the possibility of some sample dependence. It is observed that diffraction corrections are more important in the evaluation of the nonlinearity parameter than assumed for crystals of cubic symmetry.

A negative nonlinearity parameter is found to exist for quartz in the X-direction. This is a phenomenon which thus far has been observed only once before—in fused silica.

Very small nonlinearity parameters are observed in the direction corresponding to piezoelectric stiffening. The possibility exists that this is a general property of piezoelectric trigonal crystals. The nonlinearity parameter of Z-cut $LiNbO_3$ is the smallest which has been measured up to the present time and consequently Z-cut $LiNbO_3$ more closely approximates a linear solid than any other material does.

There are some indications that for a strong piezoelectrically coupled solid such as $LiNbO_3$ the piezoelectric contribution to the total effective TOE constants may be measured with the capacitive detector and thus the constant field TOE constant may be determined in the Z-direction.

CHAPTER V

SUGGESTIONS FOR FURTHER WORK

This investigation has left a number of subjects which require further study.

1. The variations in the measured values of the TOE constants of $LiNbO_3$ suggest the possibility of sample dependence. This point should be investigated further by making measurements with a number of samples from different manufacturers including both optical and transducer grade crystals.

2. There were very low level second harmonic amplitudes resulting from the essentially "linear" behavior of quartz in the X-direction and $LiNbO_3$ in the Z-direction. These directions correspond to the longitudinal mode piezoelectric direction for both crystals. With only two samples one cannot decide whether this is coincidental or is a general property of piezoelectric trigonal crystals. Further measurement with the trigonal crystals will be necessary to determine whether this is a general property. If this property should prove to be general, then it might have significant theoretical implications in the study of piezoelectric solids.

3. The measurements reported in this work were made at room temperature. Especially in $LiNbO_3$, one finds a strong temperature dependence of many elastic parameters. Therefore, measurements of the TOE constants of quartz and $LiNbO_3$ should be made as a function of temperature down to liquid helium temperature. These measurements

91

would provide valuable information about nonlinear properties of these crystals which are fundamental to a detailed theory of the solid state.

4. It has been observed that the strong piezoelectrically coupled directions provide a signal from the capacitive detector, even when no bias voltage is applied. We have not observed this behavior with materials other than piezoelectric materials. This subject is worthy of detailed investigation. It is possible that the piezoelectric third-order elastic constants could be determined by such measurements. This would give access to constant field TOE constants. Also, the $f_{ijk\ell m}$ (which have never been measured) might be separated from the piezoelectric contribution by subtracting all of the other more easily measured higher-order terms.

5. The significance to solid state physics of the (rarely occurring) negative nonlinearity parameter should be investigated further.

BIBLIOGRAPHY

BIBLIOGRAPHY

Bains, James A., Jr. "Variations of Combinations of Third-Order Elastic Constants in Germanium between 3 and 300°K," Ph.D. dissertation, The University of Tennessee, Knoxville, 1974.

Bains, James A., Jr. and M. A. Breazeale. J. Acoust. Soc. Am. $\underline{57}$, 745 (1975).

Baryshnikova, F. F. and V. E. Lyamov. Sov. Phys. Acoust. $\underline{24}$, 267 (1978).

Bateman, T., W. P. Mason, and H. J. McSkimin. J. Appl. Phys. $\underline{32}$, 928 (1961).

Birch, F. Phys. Rev. $\underline{71}$, 809 (1947).

Blackburn, Bruce D. "Ultrasonic Determination of Combinations of Small Cubic Single Crystals," Ph.D. dissertation, The University of Tennessee, Knoxville, 1981.

Breazeale, M. A. and D. O. Thompson. Appl. Phys. Lett. $\underline{3}$, 77 (1963).

Breazeale, M. A. and J. Ford. J. Appl. Phys. $\underline{36}$, 3486 (1965).

Breazeale, M. A. and J. Philip. In Physical Acoustics, edited by Warren P. Mason and R. N. Thurston (Academic Press, New York, 1983), Vol. 17.

Brugger, K. Phys. Rev. $\underline{133}$, A1611 (1964).

Carr, P. H. Phys. Rev. $\underline{169}$, 718 (1968).

Cook, W. R., Jr. and H. Jaffe. In Landolt-Börnstein Numerical Data and Functional Relationships in Science and Technology, edited by K. H. Hellwege (Springer-Verlag, Heidelberg and New York, 1979), V. 11.

Dieulesaint, E. and D. Royer. Elastic Waves in Solids (John Wiley and Sons, New York, 1980).

Farnel, G. W. Can. J. Phys. $\underline{39}$, 65 (1961).

Gauster, W. B. and M. A. Breazeale. Rev. Sci. Instrum. $\underline{37}$, 1544 (1966).

Graham, R. A. Phys. Rev. B $\underline{6}$, 4779 (1972).

Graham, R. A. J. Appl. Phys. $\underline{48}$, 2153 (1977).

Gredvits, A. A. and V. A. Krasilnikov. Sov. Phys. JETP 16, 1122 (1963).

Hankey, R. E. and D. E. Schuele. J. Acoust. Soc. Am. 48, 190 (1970).

Hearmon, R. F. S. In Landolt-Börnstein Numerical Data and Functional Relationships in Science and Technology, edited by K. H. Hellwege (Springer-Verlag, Berlin, Heidelberg, New York, 1979), Vol. 11.

Hikata, A., B. B. Chick, and C. Elbaum. J. Appl. Phys. 36, 229 (1965).

Hughes, D. S. and J. L. Kelly. Phys. Rev. 92, 1145 (1953).

Kaga, H. Phys. Rev. 172, 900 (1968).

Lazarus, D. Phys. Rev. 76, 545 (1949).

Lord Rayleigh. Proc. Roy. Soc. A84. 247 (1910).

Mathur, S. S. and P. N. Gupta. Acustica 23, 160 (1970).

McMahon, D. H. J. Acoust. Soc. Am. 44, 1007 (1965).

McSkimin, H. J., P. Andreatch, Jr., and R. N. Thurston. J. Appl. Phys. 36, 1624 (1965).

Murgaghan, F. D. Finite Deformations of an Elastic Solid (John Wiley and Sons, New York, 1951).

Musgrave, M. J. P. Proc. Roy. Soc. A226, 356 (1954).

Musgrave, M. J. P. Crystal Acoustics (Holden-Day, San Francisco, 1970).

Nakagawa, Y., K. Yamanouni, and K. Shibayama. J. Appl. Phys. 44, 3969 (1973).

Peters, R. D. "Ultrasonic Measurement of the Temperature Dependence of Copper Nonlinearity Parameters," Ph.D. dissertation, The University of Tennessee, Knoxville, 1968; ORNL-TM-2286 (1969).

Philip, J. and M. A. Breazeale. Proceedings of Institute of Electrical and Electronics Engineers Ultrasonic Symposium, 1982, p. 1022.

Philip, J. Technical Report No. 22, Office of Naval Research Contract No. N00014-81-K-0229, The University of Tennessee, Knoxville (to be published in 1983).

Rauber, A. In Current Topics in Material Science, edited by
    e. Kaldis, (North-Holland, New York and Oxford, 1978), Vol. I.

Seeger, A. and O. Buck. Naturforschg. 15a, 1056 (1960).

Spencer, E. G., P. V. Lenzo, and K. Nassau, Appl. Phys. Lett. 7, 67
    (1965).

Smith, R. T. and F. S. Welsh. J. Appl. Phys. 42, 2219 (1971).

Stern, R. and R. T. Smith. J. Acoust. Soc. Am. 44, 640 (1968).

Thurston, R. N. In Physical Acoustics, edited by Warren P. Mason
    and R. N. Thurston (Academic Press, 1964), V. 1A.

Thurston, R. N., and K. Brugger, Phys. Rev. A133, 1604 (1964).

Thurston, R. N. and M. J. Shapiro. J. Acoust. Soc. Am. 41, 1112
    (1967).

Thurston, R. N., H. J. McSkimin, and P. Andreatch, Jr. J. Appl. Phys.
    37, 267 (1966).

Truell, R., C. Elbaum, and B. B. Chick. Ultrasonic Methods in Solid
    State Physics (Academic Press, New York, 1969).

Voigt, W. Lehrbuch der Kristallphysik (Teubner, Leipzig and Berlin,
    1928).

Warner, A. W., M. Ohoe, and G. A. Coquin. J. Acoust. Soc. Am. 42,
    1223 (1967).

William, J. and J. Lamb. J. Acoust. Soc. Am. 30, 308 (1958).

Yost, W. T. "An Ultrasonic Investigation of the Magnitude and
    Temperature Dependence of the Nonlinearity Parameter of Ger-
    manium and Fused Silica," Ph.D. dissertation, The University of
    Tennessee, Knoxville, 1972.

Zarembo, L. K and V. A. Krasilnikov. Sov. Phys. Usp. 13, 1778 (1971).

REPORTS DISTRIBUTION LIST FOR ONR PHYSICS PROGRAM OFFICE
UNCLASSIFIED CONTRACTS

Director   3 copies
Defense Advanced Research Projects Agency
Attn: Technical Library
1400 Wilson Blvd.
Arlington, Virginia 22209

Office of Naval Research   3 copies
Physics Program Office (Code 421)
800 North Quincy Street
Arlington, Virginia 22217

Office of Naval Research   1 copy
Director, Technology (Code 200)
800 North Quincy Street
Arlington, Virginia 22217

Naval Research Laboratory   3 copies
Department of the Navy
Attn: Technical Library
Washington, DC 20375

Office of the Director of Defense   3 copies
   Research and Engineering
Information Office Library Branch
The Pentagon
Washington, DC 20301

U. S. Army Research Office   2 copies
Box 12211
Research Triangle Park
North Carolina 27709

Defense Technical Information Center   12 copies
Cameron Station
Alexandria, Virginia 22314

Director, National Bureau of Standards   1 copy
Attn: Technical Library
Washington, DC 20234

Commanding Officer   3 copies
Office of Naval Research Western Regional Office
1030 East Green Street
Pasadena, California 91101

Commanding Officer   3 copies
Office of Naval Research Eastern/Central Regional Office
666 Summer Street
Boston, Massachusetts 02210

```
Director                                              1 copy
U. S. Army Engineering Research
  and Development Laboratories
Attn:  Technical Documents Center
Fort Belvoir, Virginia  22060

ODDR&E Advisory Group on Electron Devices             3 copies
201 Varick Street
New York, New York 10014

Air Force Office of Scientific Research               1 copy
Department of the Air Force
Bolling AFB, D. C. 22209

Air Force Weapons Laboratory                          1 copy
Technical Library
Kirtland Air Force Base
Albuquerque, New Mexico 87117

Air Force Avionics Laboratory                         1 copy
Air Force Systems Command
Technical Library
Wright-Patterson Air Force Base
Dayton, Ohio  45433

Lawrence Livermore Laboratory                         1 copy
Attn:  Dr. W. F. Krupke
University of California
P.O. Box 808
Livermore, CAlifornia 94550

Harry Diamond Laboratories                            1 copy
Technical Library
2800 Powder Mill Road
Adelphi, Maryland  20783

Naval Air Development Center                          1 copy
Attn:  Technical Library
Johnsville
Warminster, Pennsylvania  18974

Naval Weapons Center                                  1 copy
Technical Library (Code 753)
China Lake, California  93555

Naval Training Equipment Center                       1 copy
Technical Library
Orlando, Florida  32813

Naval Underwater Systems Center                       1 copy
Technical Center
New London, Connecticut  06320
```

LME

-8